Electronic Supplementary Material (ESI) for RSC Advances.

Supporting Information

Heterologous expression of the cryptic *mdk* gene cluster and structural revision of maduralactomycin A

Table of Figures

Table of Tables

Table S1 .Composition of culture media

DNPM [1]	40.0 g/L Dextrin, 7.48 g/L pepton from soy, 5.0 g/L yeast extract, 21.0 g/L MOPS 3-(N-morpholino)propanesulfonic acid
ISP2[2]	4 g/L yeast extract 10 g/L malt extract 4 g/L glucose
LB	(Carl Roth, Germany)
SOB	(Carl Roth, Germany)
CASO	(Carl Roth, Germany)

Table S2. Growth conditions for strains used in this study.

Strain	Medium/Antibiotic	
E. coli/ mdk BGC containing plasmid (SPIRO BGC)	LB (Carl Roth, Germany), + apramycin (50 µg/mL)	37 °C at 160 rpm
E. coli/ΔacrR/ ΔKS (mdk BGC containing plasmid with knocked out regulator)	LB (Carl Roth, Germany), + spectinomycin (50 µg/mL)	37 °C at 160 rpm
E. coli HB101:prK2013	LB (Carl Roth, Germany), + kanamycin (50 µg/mL)	antibiotic was added at a cultivation temperature of 30 °C.
E. coli BW25113/piJ790	LB, SOB (Carl Roth, Germany) + chloramphenicol (25 µg/mL)	30°C, 150 rpm
E. coli BW25113/piJ790/SPIRO BGC	LB, SOB (Carl Roth, Germany) + chloramphenicol (25 µg/mL) + apramycin (50 µg/mL)	30°C, 150 rpm
E. coli BW25113/piJ790/SPIRO_ΔacrR	LB, SOB (Carl Roth, Germany) + chloramphenicol (25 µg/mL) + spectinomycin (50 µg/mL)	30°C, 150 rpm
E. coli ET12567 pUZ8002	LB (Carl Roth, Germany) + kanamycin (25 µg/mL) + chloramphenicol (25 µg/mL)	37 °C at 160 rpm
E. coli ET12567 pUZ8002 SPIRO BGC	LB (Carl Roth, Germany) + kanamycin (25 µg/mL) + chloramphenicol (25 µg/mL) + apramycin (50 µg/mL)	37 °C at 160 rpm
E. coli DH5α pIJ778	LB (Carl Roth, Germany) + spectinomycin (50 µg/mL)	37 °C at 160 rpm
Streptomyces albus J1074	CASO media (Carl Roth, Germany)	28°C, 140 rpm
Streptomyces coelicolor M1146	CASO media (Carl Roth, Germany)	28°C, 140 rpm
Streptomyces lividans TK24	CASO media (Carl Roth, Germany)	28°C, 140 rpm
Streptomyces albus J1074 / SAS116 α	CASO media (Carl Roth, Germany) DNPM + apramycin (50 µg/mL)	28°C, 140 rpm
Streptomyces coelicolor M1146/ 1.8PI	CASO media (Carl Roth, Germany) DNPM + apramycin (50 µg/mL)	28°C, 140 rpm
Streptomyces albus J1074 / SaΔacrR	CASO media (Carl Roth, Germany) DNPM + spectinomycin (100 µg/mL)	28°C, 140 rpm
Streptomyces lividans TK24 / 1.32PISL	CASO media (Carl Roth, Germany) ISP2 + apramycin (50 µg/mL)	28°C, 140 rpm

Table S3. Strains and plasmids used in this study

Name	**Type**	**Reference**
Streptomyces albus J1074	Wild type, heterologous host	3,4
Streptomyces coelicolor M1146	Wild type, heterologous host	5
Streptomyces lividans TK24	Wild type, heterologous host	6
SPIRO Plasmid	*mdk* containing pDualP vector: Plasmid carrying the putative *mdk* cluster	Varigen Biosciences Now: Terra Bioforge: Synthetic Biology Platform
SPIRO_ΔacrR	Plasmid carrying the putative *mdk* cluster with knocked out regulators	This study
Streptomyces albus SAS116α	*Streptomyces albus* J1074 carrying the SPIRO plasmid	This study
Streptomyces coelicolor 1.8PI	*Streptomyces coelicolor* M1146 carrying the SPIRO plasmid	This study
Streptomyces lividans 1.32PISL	*Streptomyces lividans* TK24 carrying the SPIRO plasmid	This study
E. coli HB101:prK2013	*E. coli* carrying plasmid for conjugative transfer in triparental conjugation	7,8
E. coli ET12567 pUZ8002	*E. coli* for methylation free conjugative transfer	9,10
E. coli ET12567 pUZ8002 SPRIO BGC	*E. coli* for methylation free conjugative transfer carrying the SPIRO plasmid	This study
E. coli/ mdk BGC containing plasmid (SPIRO BGC)	*E. coli* Bact.Opt. 2.0 carrying the SPIRO plasmid	Varigen Biosciences
E. coli DH5α pIJ778	*E. coli* carrying the Spectinomcin resistance	11
E. coli BW25113/piJ790	*E. coli* carrying the Plasmid for λ Red recombination	12,13
E. coli BW25113/piJ790/SPIRO BGC	*E. coli* carrying the Plasmid for λ Red recombination and the SPIRO plasmid (for recombination reaction)	This study
E. coli BW25113/piJ790/SPIRO_ΔacrR	*E. coli* carrying the mutated SPIRO plasmid (knockout of regulators)	This study
E. coli BW25113/piJ790/ SPIRO_ΔKS	*E. coli* carrying the mutated SPIRO plasmid (knockout of Ketosynthase)	This study

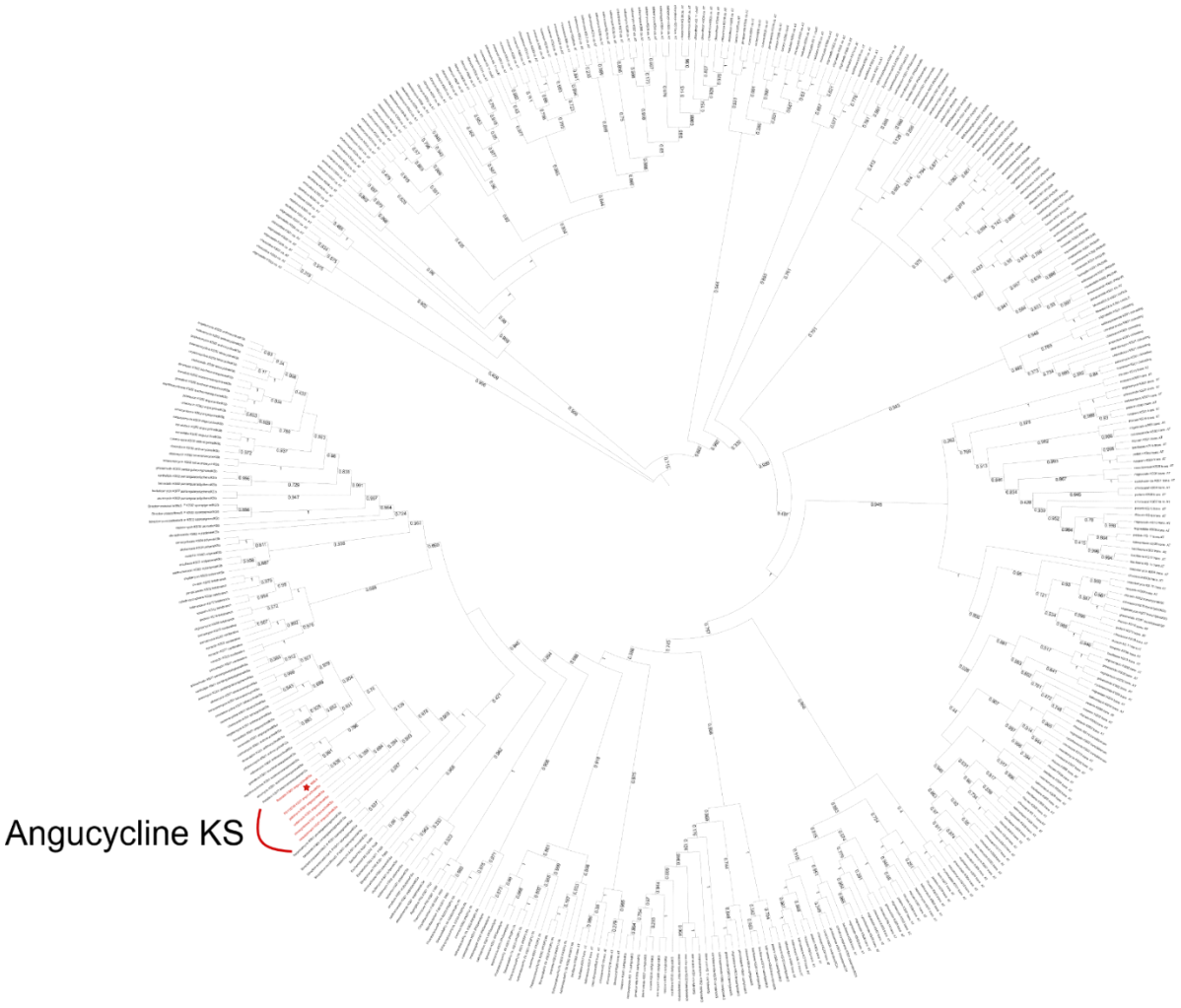

Figure S1. Phylogenetic tree of the putative ketosynthase of the *mdk* cluster MdkA created with NaPDoS2. The red branch of the tree is the branch where MdkA was placed, all neighboring ketosynthases are associated with angucycline gene clusters. MdkA is marked with a red star.

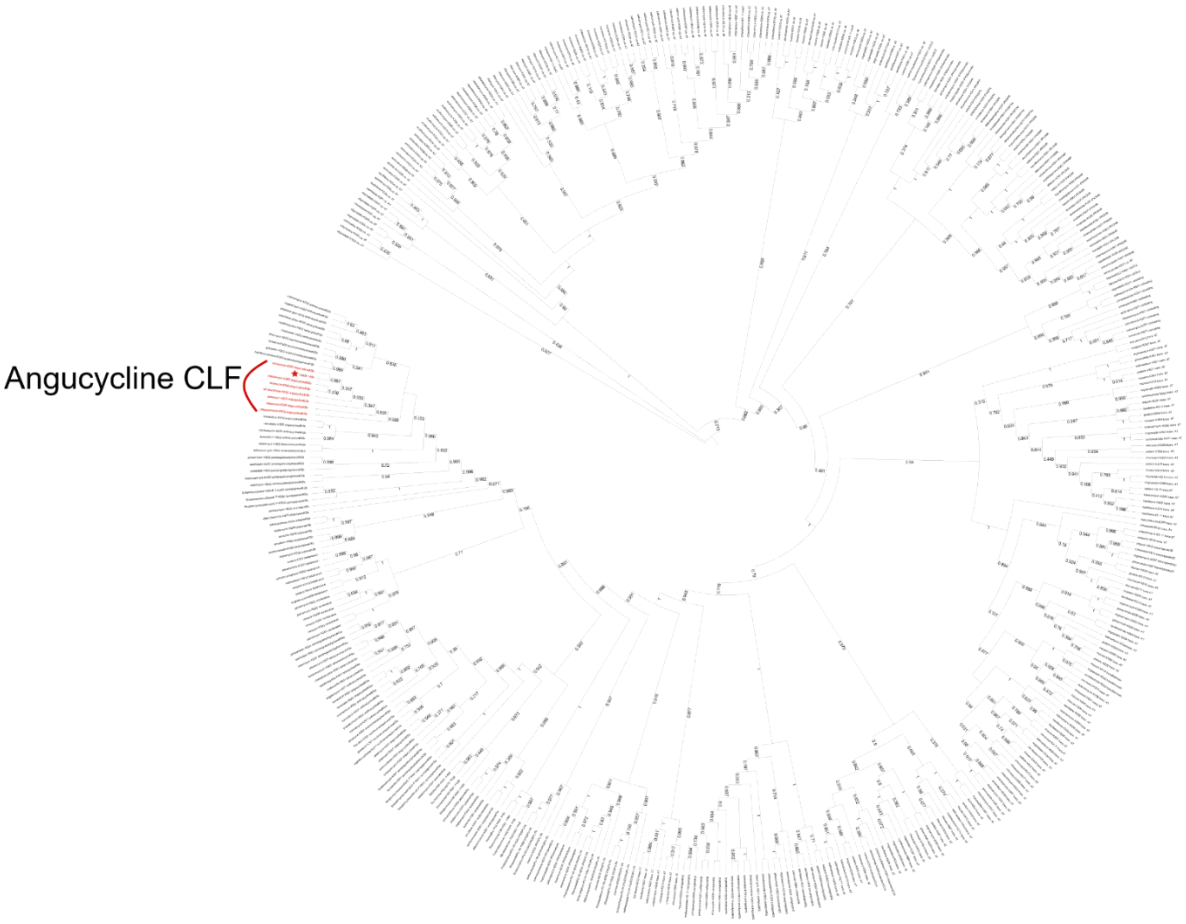

Figure S2. Phylogenetic tree of the putative chain length factor (CLF) of the *mdk* cluster MdkB created with NaPDoS2. The red branch of the tree is the branch where MdkB was placed, all neighboring CLF's are associated with angucycline gene clusters. MdkB is marked with a red star.

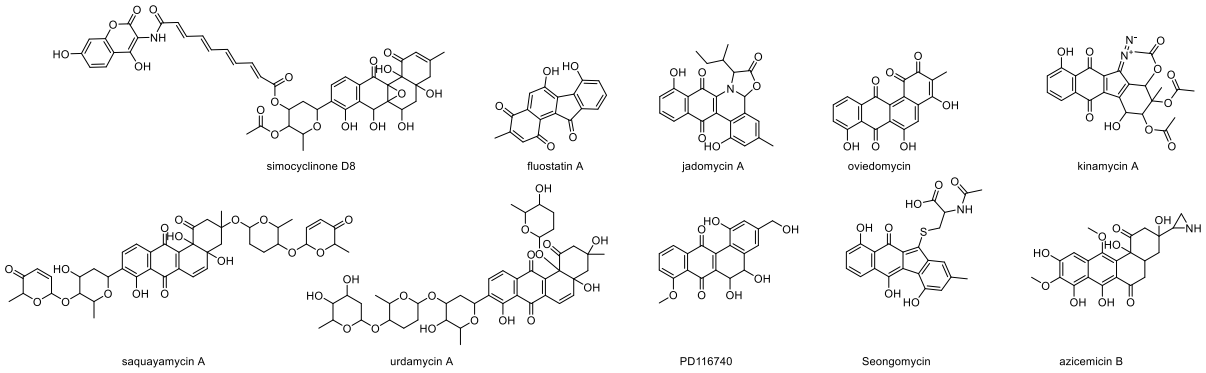

Figure S3. Structures of angucycline products correlating to depicted genes within the phylogenetic tree.

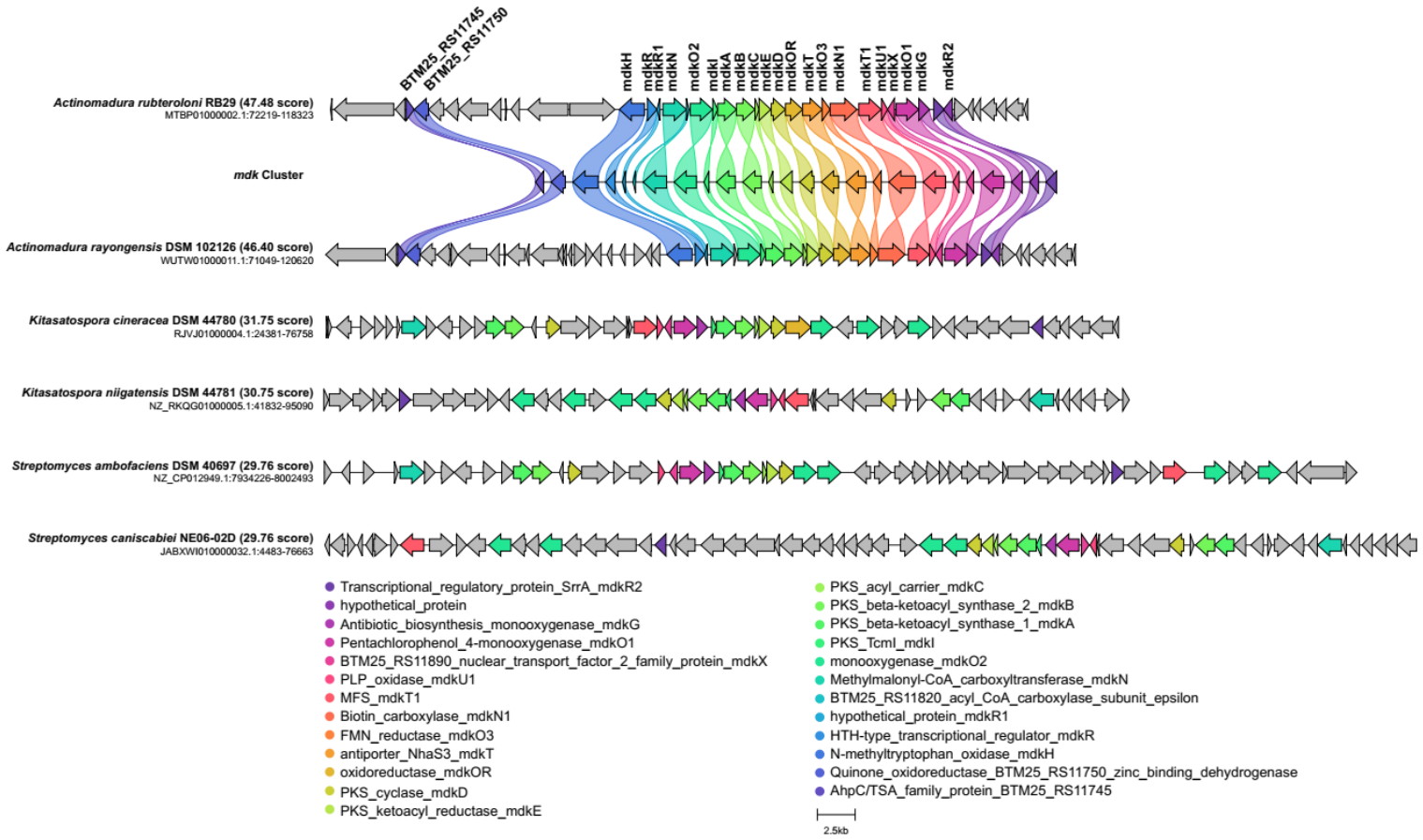

Figure S4. Cblaster analysis using the *mdk* gene cluster sequence as query sequence. Five dene clusters with similar gene arrangement and identity (threshold of 30% identity) are depicted and homologous gene sequences are shown in the same color code. Annotation of genes with the respective colour code are shown at the bottom

Table S4. PCR primers used in this study

Name and Purpose	**Sequence (5'-3')**
ΔacrR left (oligo for generating the resistance cassette for mutation of regulators)	GCACCGTGTAGACTCCCAGACGGAAGGAGATTCCGGATGATTCCGGGGATCCGTCGACC
ΔacrR right (oligo for generating the resistance cassette for mutation of regulators)	CCGCAGCGGTTCAGTTTCTCTCAACAGGAAGTTCACATGTGTAGGCTGGAGCTGCTTC
test_primer_delta_forward (verification of mutation of regulator)	AGATCTGCGGACACTTCCAC
test_primer_delta_reverse (verification of mutation of regulator)	GCACGAGTGACTCCTGTAGG
Out_cluster_Right_forward (OCR) (verification presence of plasmid backbone)	GTCCCTCTGTTTTTCGCACG
Out_cluster_Right_reverse (OCR) (verification presence of plasmid backbone)	GTATCGGCCGAGTGGTTTCA
Out_cluster_Left_Forward (OCL) (verification presence of plasmid backbone)	CTCAACGCTATCAGGCGGA
Out_cluster_Left_reverse (OCL) (verification presence of plasmid backbone)	CGCATCGGTGGCTCCTTTTT
OutRight_LONG_Forward primer (ORL) (verification presence of plasmid backbone)	GATGTTCTACCCCGACGTGC
OutRight_LONG_Reverse primer (ORL) (verification presence of plasmid backbone)	TGGAGATCCAGCCCGGATAG
recA_S_coelicolor_forward (positive control for genomic DNA in *S. coelicolor*)	CACTGAAGTTCTACGCCTCG
recA_S_coelicolor_reverse (positive control for genomic DNA in *S. coelicolor*)	TTGTCCTTCAGGAAGTTGCG

Table S5. PCR conditions used for verification of gene cluster

Step	**Temperature [°C]**	**Duration**
Heat Lid	110	
Initial Melting	98	30 s
Start Cycle		*35 x*
Melting	98	15 s
Annealing	64	30 s
Elongation	72	30 s
End Cycle		
Final Elongation	72	5 min.
Store	4	∞

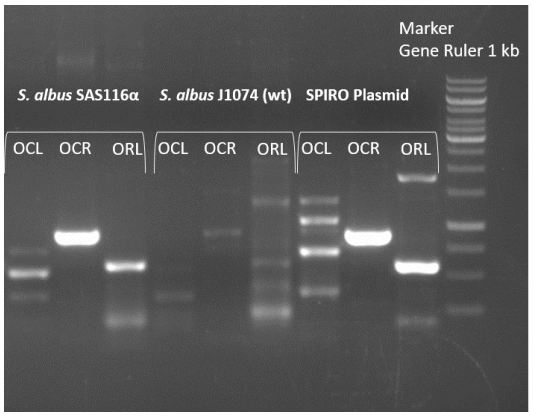

Figure S5 Gel chromatogram to verify the presence of the SPIRO plasmid in *S. albus* J1074.

Left: Samples of *S. albus* carrying the SPIRO plasmid, middle: *S. albus* wildtype (negative control); right: SPIRO plasmid (positive control).

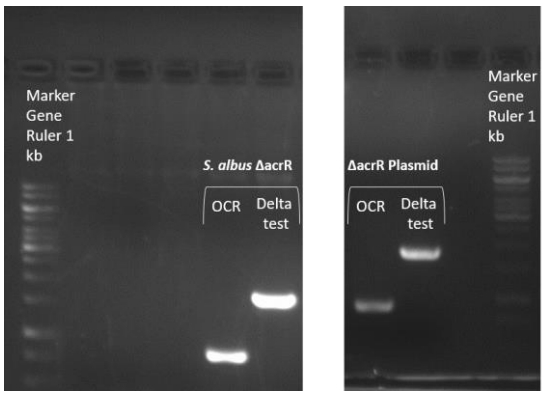

Figure S6. Gel chromatogram to verify the presence of the mutated plasmid (ΔacrR) in *S. albus* J1074.
Left: Samples of genomic DNA from strain carrying the mutated plasmid; Right: Samples of DNA of isolated ΔacrR plasmid.

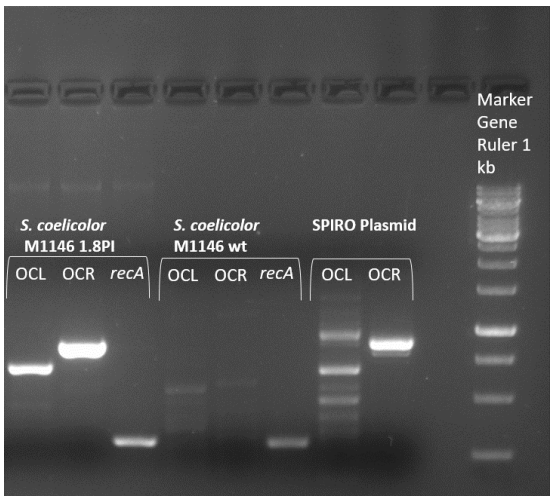

Figure S7. Gel chromatogram to verify the presence of the SPIRO plasmid in *S. coelicolor* M1146.
Left: samples from strain carrying plasmid; middle: samples of wildtype (negative control); right: plasmid DNA (positive control). The recA gene was used as a reference sequence to analyze for the presence of genomic DNA.

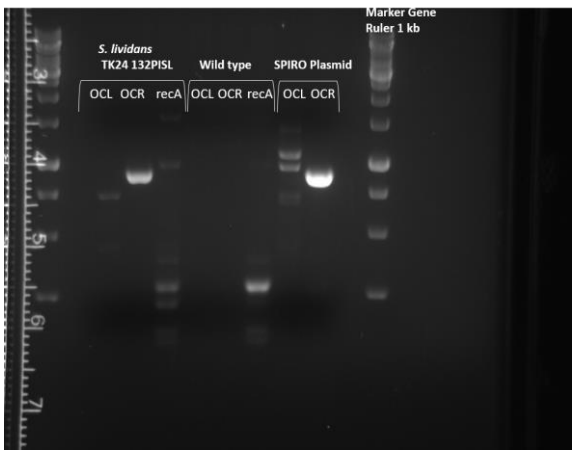

Figure S8. Verification of SPIRO plasmid in *S. lividans* TK24.

Left strain carrying plasmid, middle wild type (negative control), right plasmid DNA (positive control). The recA gene was used as a reference sequence to analyze for the presence of genomic DNA.

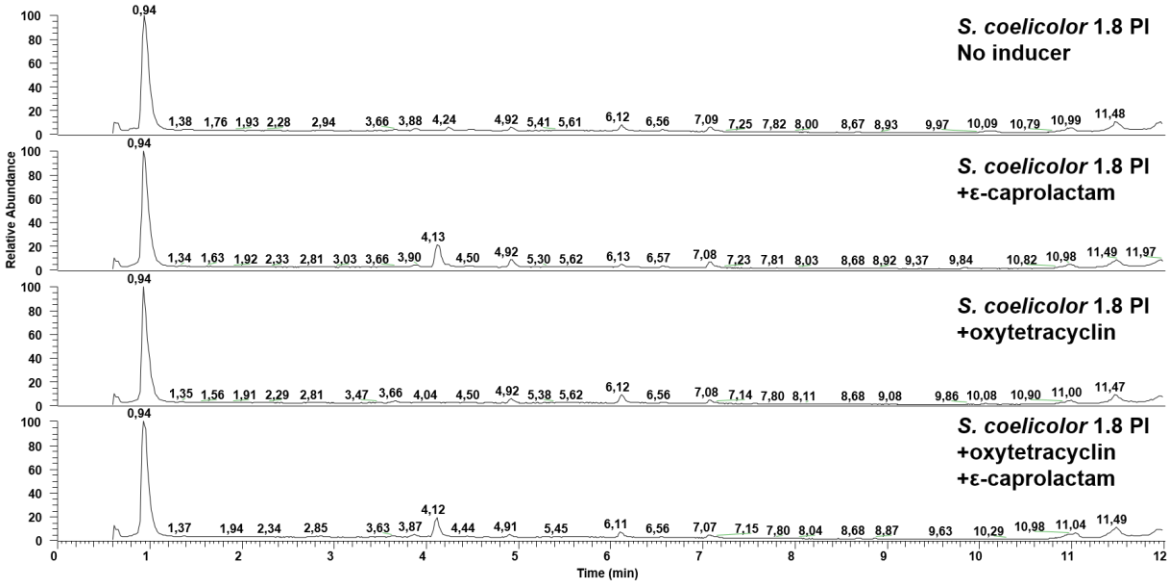

Figure S9. Total ion chromatogram of culture extracts of *S. coelicolor* strains carrying the *mdk* cluster obtained after treatment with different combinations of inducer (oxytetracycline and ε-caprolactam).

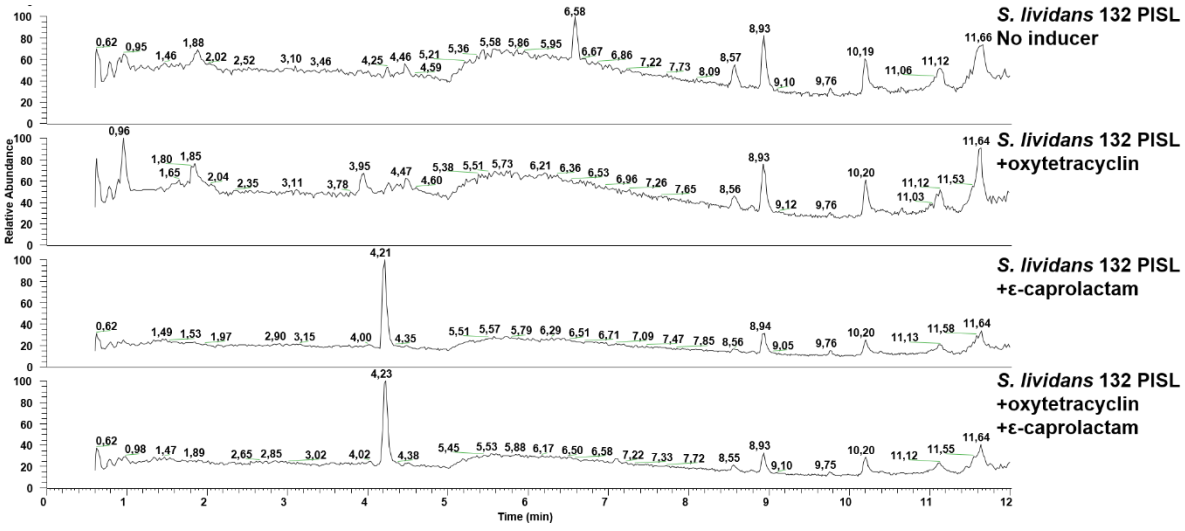

Figure 10. Total ion chromatogram of culture extracts of *S. lividans* strains carrying the *mdk* cluster obtained after treatment with different combinations of inducer (oxytetracycline and ε-caprolactam).

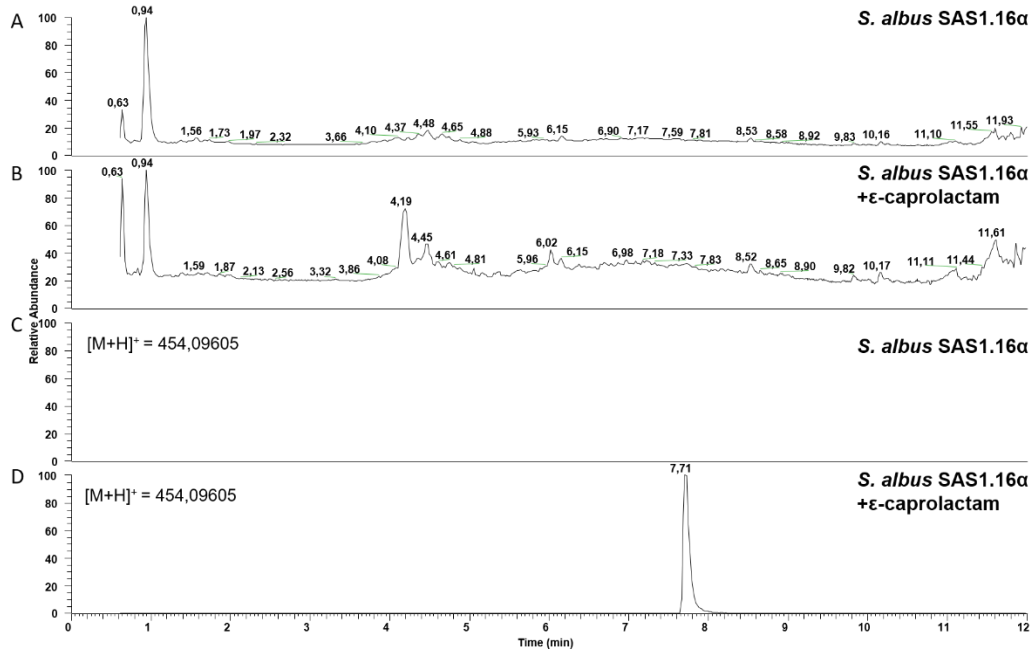

Figure S11. Total ion chromatograms (A,B) and extracted ion chromatograms (C,D) of culture extracts of *S. albus* carrying the *mdk* cluster obtained after treatment with different inducer combinations.

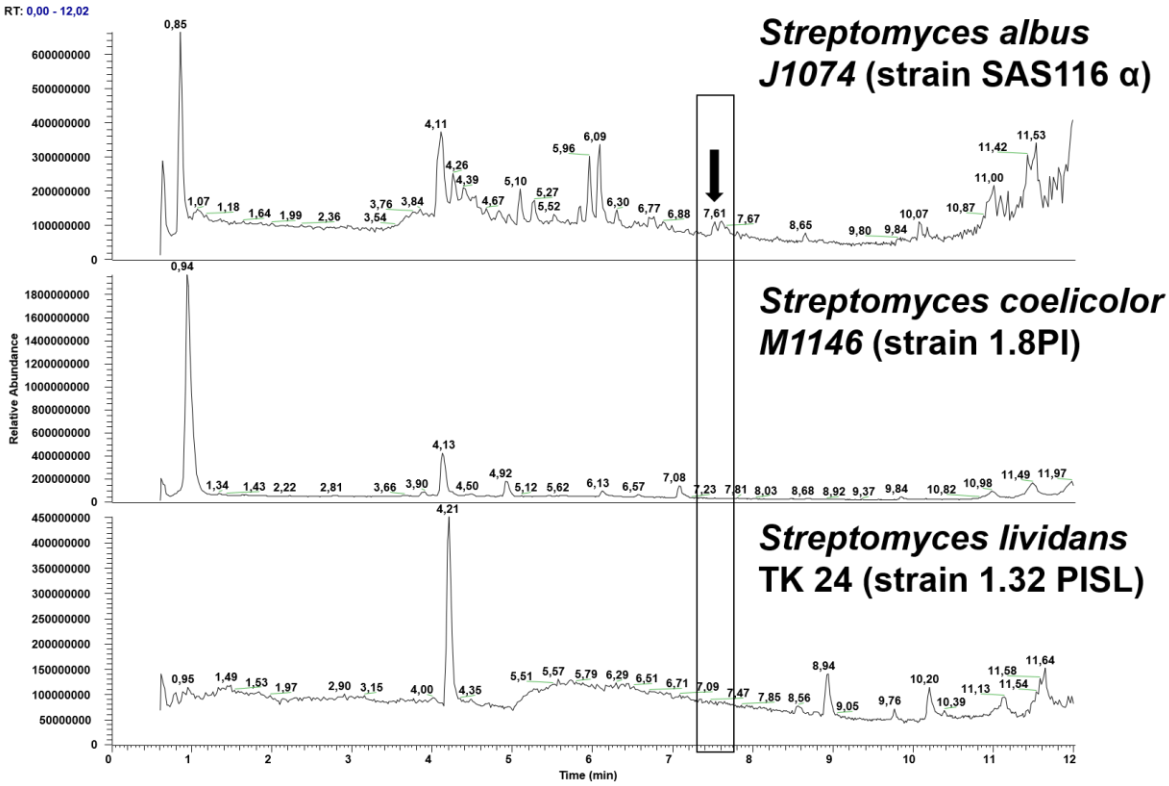

Figure S12. Total ion chromatograms of cultivation experiments with different expression strains carrying the *mdk* cluster in the presence of the inducer ε-caprolactam. Retention time and peak with *m/z* =454.0961 [M+H$^+$] is marked with an arrow.

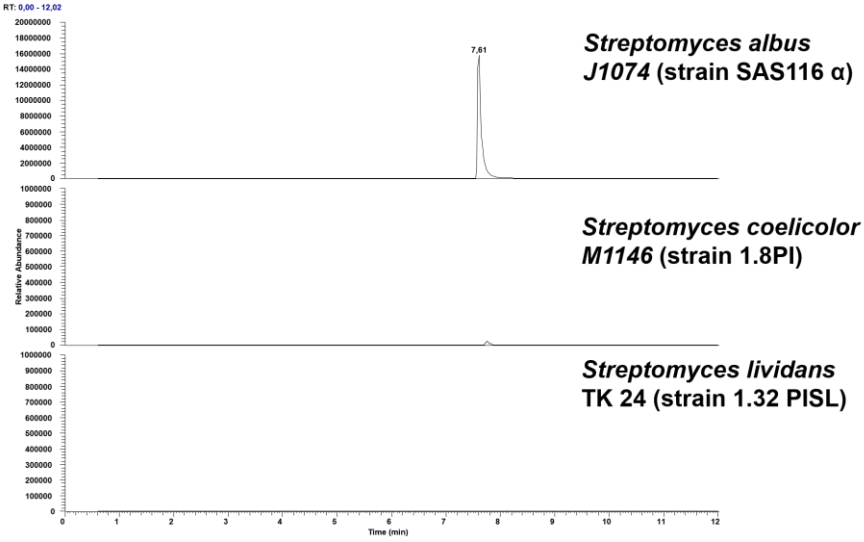

Figure S13. Extracted ion chromatogram (*m/z* =454.0961 [M+H$^+$]) using LC-MS/MS data from culture extracts of different expression strains. The respective expression host and the strain carrying the *mdk* BGC are named on the right side of the chromatograms.

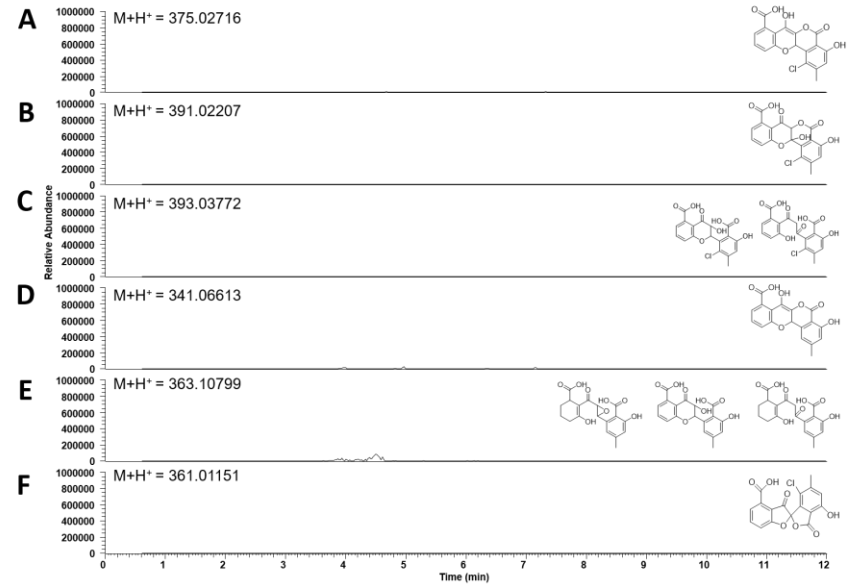

Figure S14. Extracted ion chromatogram using LC-MS/MS data from culture extracts of the expression strain *S. albus* SAS116α. Searched *m/z* values that could correspond to maduralactomycin-like core structures (A-F) are depicted on the left side of the chromatogram.

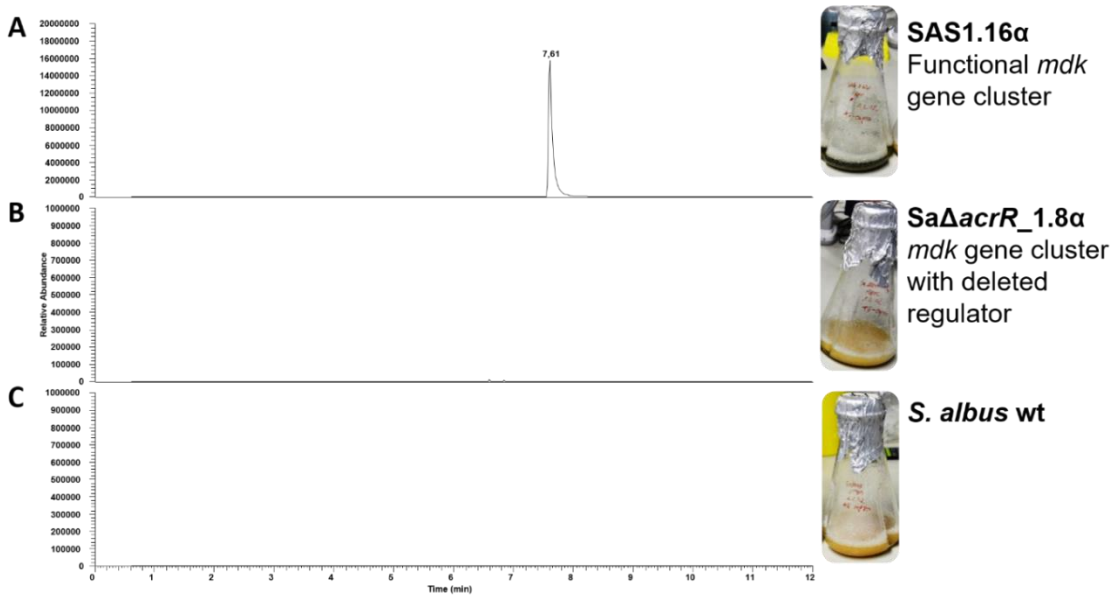

Figure S15. Extracted ion chromatogram (*m/z* =454.0961 [M+H$^+$]) using LC-MS/MS data retrieved from culture extracts of the expression strain *S. albus* SAS116α carrying the functional *mdk* cluster, modified strain SaΔacrR_1.8α and *S. albus J1074* wildtype.

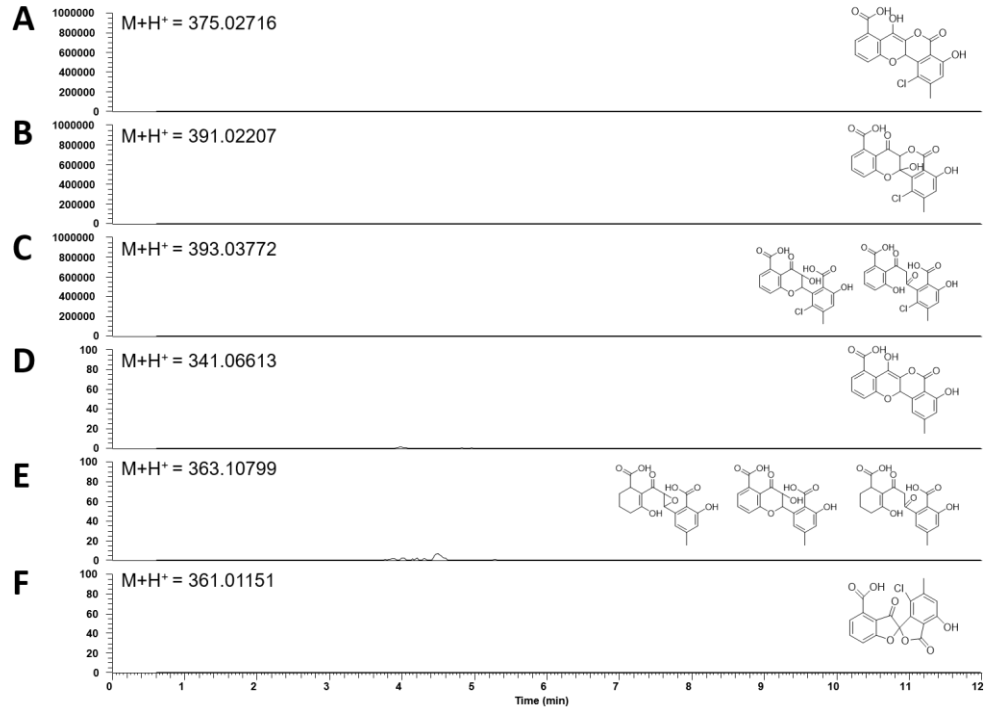

Figure S16. Extracted ion chromatograms of *m/z* values corresponding to putative maduralactomycin derivatives (A-F) that could be produced by the modfied strain SaΔacrR. The respective *m/z* [M+H$^+$] values as well as the respective structures are found in each line (A-F).

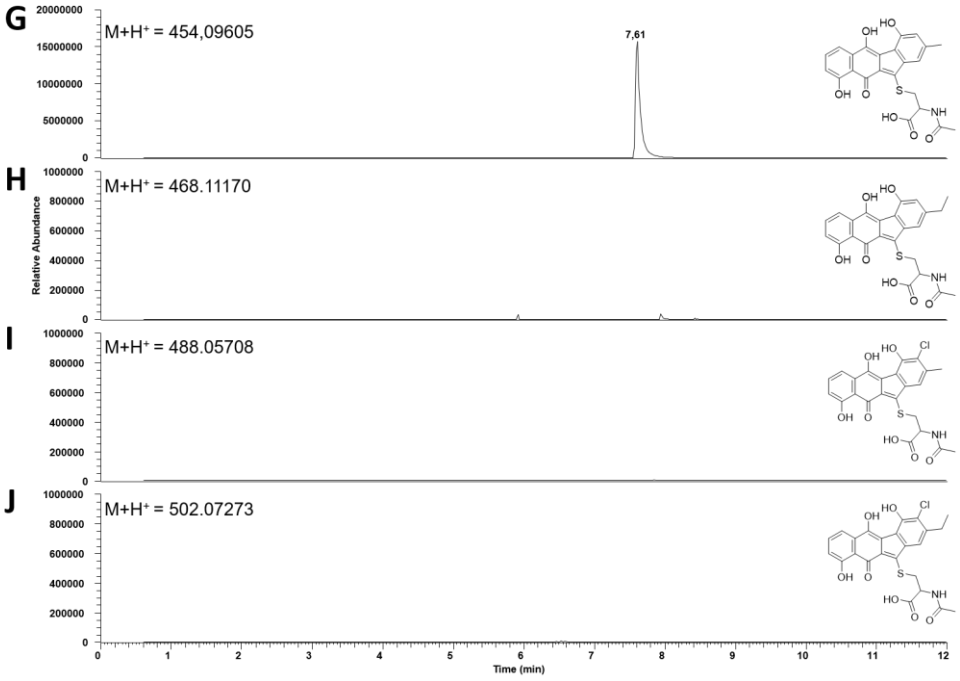

Figure S17. Extracted ion chromatogram of *m/z* values corresponding to putative seongomycin derivatives (G-J) that could be produced by strain SAS116α. The respective *m/z* [M+H$^+$] values as well as the respective structures are found in each line (G-J)

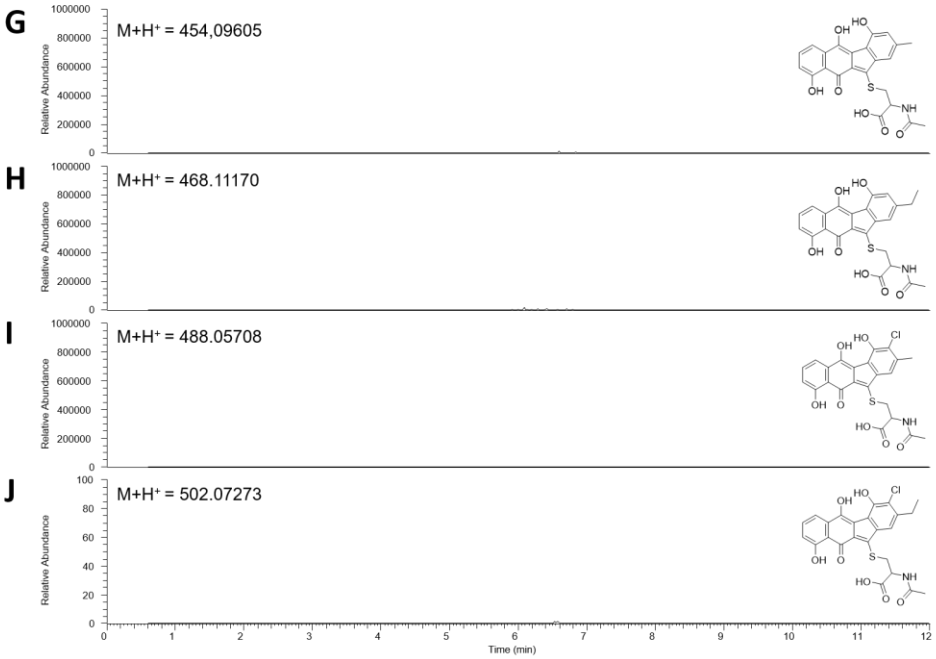

Figure S18. Extracted ion chromatogram of *m/z* values corresponding to putative seongomycin derivatives that could be produced by strain SaΔacrR. The respective *m/z* [M+H$^+$] values as well as the respective structures are found in each line (G-J)

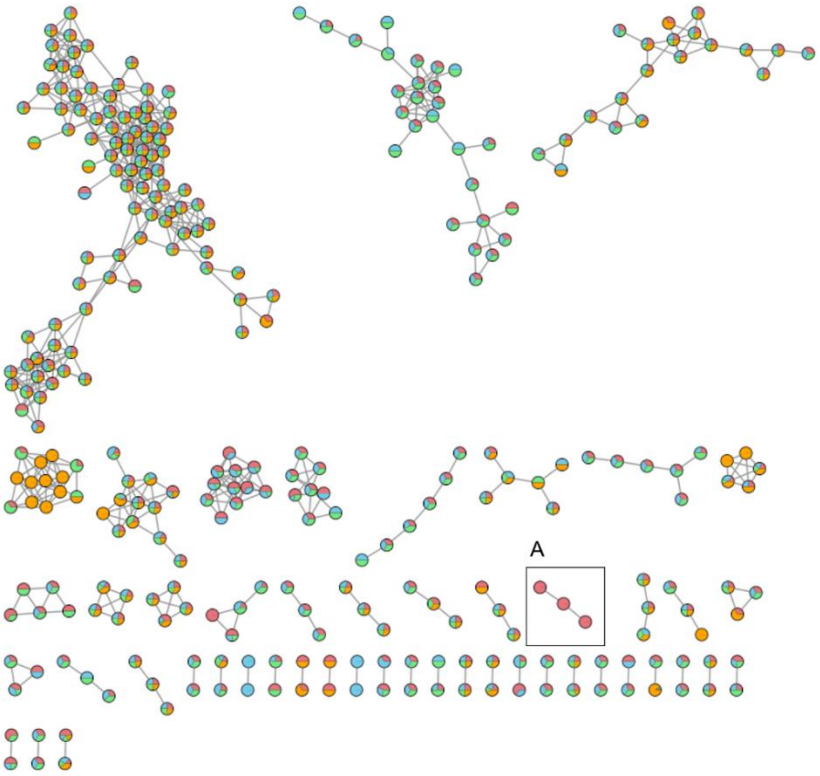

Figure S19. Exemplary GNPS-based network analysis of 10% MeOH SPE Fraction without self-loops. Red SAS116, Blue ΔSAS116, Green SAS WT, Orange blank. Cluster A marks the seongomycin cluster.

Table S6. Summary of GNPS nodes exclusively occurring in strain *S. albus* J1074/SAS116 α

m/z	Int [10^6]	RT [min]	SumForm[$M+H^+$]	Comments
Cluster A (10% MeOH SPE Fraction)				
454.094	22.6	7.74	C23H20O7NS	Seongomycin + ionization cluster? Also traces in ΔSAS (10^4)
468.074	1.11	7.74	C23H18O8NS	13.98 to 454.094 (+O -H_2)
452.079	2.77	7.74	C23H18O7NS	15.995 (Oxygen) to 468.074
Self-Loops (10% MeOH SPE Fraction)				
190.086	0.79	4.08-4.2	C11H12O2N	Broad and background
472.171	0.99	5.68	C23H26O8N3	
245.099		1-12		Background, also in 100%
426.165	1.37	5,57; 6.0	C22H24O6N3?	2 peaks, MS +2 and -2 Pattern caused by overlap with other compound? (Pseudohalogen?)
453.165	0.76	4.73; 4.87	C24H25O7N2	2 Peaks
369.096	1.38	6.26	C20H17O7	
482.144	1.71	5.20	C25H24O9N	Not clear sum formula
201.073		1-12		Background
261.130		1-12		Background, also in 100%
Self-Loops (100% MeOH SPE Fraction)				
460.139	1.73	7.05	C27H26O2NS2	high M+2 → indicates Sulfur
245.099		1-12		Background
189.052		1-12		Background
454.095	11.0	7.74	C23H20O7NS	Seongomycin
215.089		1-12		Background
261.131		1-12		Background, Also in 10%
1109.580	1.55	7.38	$C_{60}H_{84}N_2O_{18}$	Overlap of Candicidin derivatives
289.125		1-12		Background
517.370	5.43	10.93	C24H49O6N6	
493.139	0.47	6.76; 7.05	C29H21O6N2	2 Peaks
442.259	0.50	6.94; 7.77	C19H43O2N3S3	2 Peaks
245.099		1-12		Background, also in 10%

Table S7. Summary of GNPS nodes exclusively occurring in *S. albus* SaΔacrR

m/z	Int [10^6]	RT [min]	SumForm[$M+H^+$]	Comments
Cluster B1 (10% MeOH SPE Fraction)				
680.227	7.48	0.97; 1.52	C26H34O13N9	2 Peaks
694.243	1.96	0.97; 2.05	C27H36O13N9	14.016 CH_2
Cluster B2 (10% Fraction)				
694.243	1.96	0.97; 2.05	C27H36O13N9	Duplicate Cluster of B1 2nd Peak?
680.227	7.48	0.97; 1.52	C26H34O13N9	Duplicate Cluster of B1 2nd Peak?
Self-Loops (10% MeOH SPE Fraction)				
365.191	2.11	0.93; 1.36	C15H29O8N2	
443.333	27.1	11.47	C21H43O4N6	
473.344	8.44	10.96	C22H45O5N6	
351.176	4.00	0.82	C14H27O8N2	Flowthrough
Cluster C1 (100% MeOH SPE Fraction)				
694.243	1.70	0.99; 2.04	C27H36O13N9	-14.014 to 680.229, see **B1-2**
664.233	2.39	0.97; 1.61	C26H34O12N9	-CH_2O to 694.243 ?
680.229	6.05	0.97; 1.52	C26H34O13N9	15.996 (Oxygen) to 664.233; see **B1-2**
1393.620	0.019	4.92	?	Low intensity
Cluster C2 (100% MeOH SPE Fraction)				
694.243	1.70	0.99; 2.04	C27H36O13N9	Duplicate from C1 missing 1393.62
680.228	6.05	0.97; 1.52	C26H34O13N9	Duplicate from C1 missing 1393.62
664.233	2.39	0.97; 1.61	C26H34O12N9	Duplicate from C1 missing 1393.62
Cluster D (100% MeOH SPE Fraction)				
335.181	0.84	8.11	C14H27O7N2	Flowthrough, ionization cluster
351.176	23.7	0.82	C14H27O8N2	15.995 (Oxygen) to 335.181
365.191	14.4	0.93	C15H29O8N2	14.015 (CH_2) to 351.176
Cluster E (100% Fraction))				
898.611	1.07	7.62	C47H80N9O8	Surugamide B,C,D
912.627	7.86	7.82	C48H82N9O8	14.016 (CH_2) to 898.611 Surugamide A
Self-Loops (100% MeOH SPE Fraction)				
458.188	0.57	3.06	C18H28O9N5?	
473.086	0.73	6.68; 8.08	C19H21O14	2 Peaks
566.203	0.36	5.16; 5.33	C31H28O6N5	2 small peaks
299.642	0.51	3.52; 3.84	No hits	2 peaks
480.775	1.10	5.21; 5.31	No hits	2 peaks
259.120	0.59	9.89	?	
374.193	0.09	6.60	C12H24O5N9?	traces
468.278	1.88	8.40	C29H34ON5?	
215.089		1-12		Background
261.131		1-12		Background

Table S8. Summary of GNPS nodes shared by SAS 116 α and SaΔacrR

m/z	Int [10^6]	RT [min]	SumForm[$M+H^+$]	Comments
Cluster F (100% MeOH SPE Fraction)				
573.303	0.31	8.23	C27H45O11N2	
914.435	0.39	8.23	?	
900.420	0.55	7.77	?	-14.015 CH_2 to 914.435
721.185	0.69	7.80	C31H29O13N8?	
897.408	0.39	8.23	C41H57O13N10	14.015 to 883.393
883.393	1.84	7.77	C40H55O13N10	Occurs In wildtype
869.377	0.53	7.42	C39H53O13N10	14.016 CH_2 to 883.393
911.424	0.5	8.64	C42H59O13N10	14.016 CH_2 to 897.408
Cluster G (100% MeOH SPE Fraction)				
611.297	3.04	6.23	?	
373.219	7.13	4.28	C15H29O5N6	
485.272	5.20	5.68	C21H37O7N6	
486.303	63.1	4.28	C21H40O6N7	
Cluster H (100% MeOH SPE Fraction)				
632.254	0.98	5.72	C28H42O15N	Broad
374.108	1.61	5.72	C15H20O10N	Broad
356.097	1.95	5.72	C15H18O9N	
416.118	4.48	6.10	C17H22O11N	Occurs also in Wildtype
Cluster I (100% MeOH SPE Fraction)				
548.319	0.13	5.46	C25H46O10N3	Alternative C26H42O6N7
649.367	0.14	5.31	C29H53O12N4?	
706.387	0.22	4.5; 5.19	C31H56O13N5	2 Peaks, Traces
Cluster J (100% MeOH SPE Fraction)				
508.285	1.93	4.28	?	
993.579	0.47	4.28	?	Traces
Cluster K (100% F MeOH SPE Fraction)				
905.375	0.43	7.77	?	
919.390		8.23	?	14.015 (CH_2) to 905.375
Cluster L (100% MeOH SPE Fraction)				
1009.540	0.016	6.71	?	traces
1025.520	?	?	?	
Cluster M (100% MeOH SPE Fraction)				
484.273	0.43	8.41	C29H34O2N5?	
482.257	0.75	8.32	C29H32O2N5	-2.016 (H_2, Double bond) 484.273

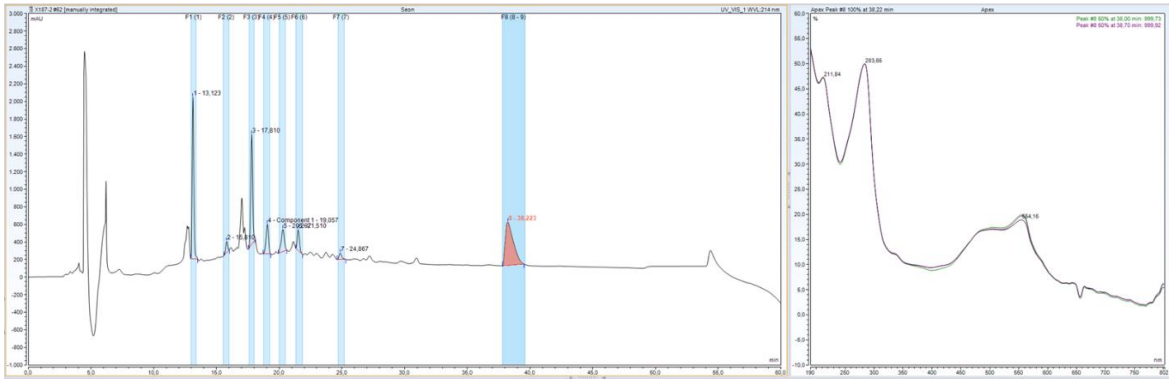

Figure S20. Preparative HPLC chromatogram of the extract containing seongomycin (left), UV absorption and HRMS spectrum of purified seongomycin (right).

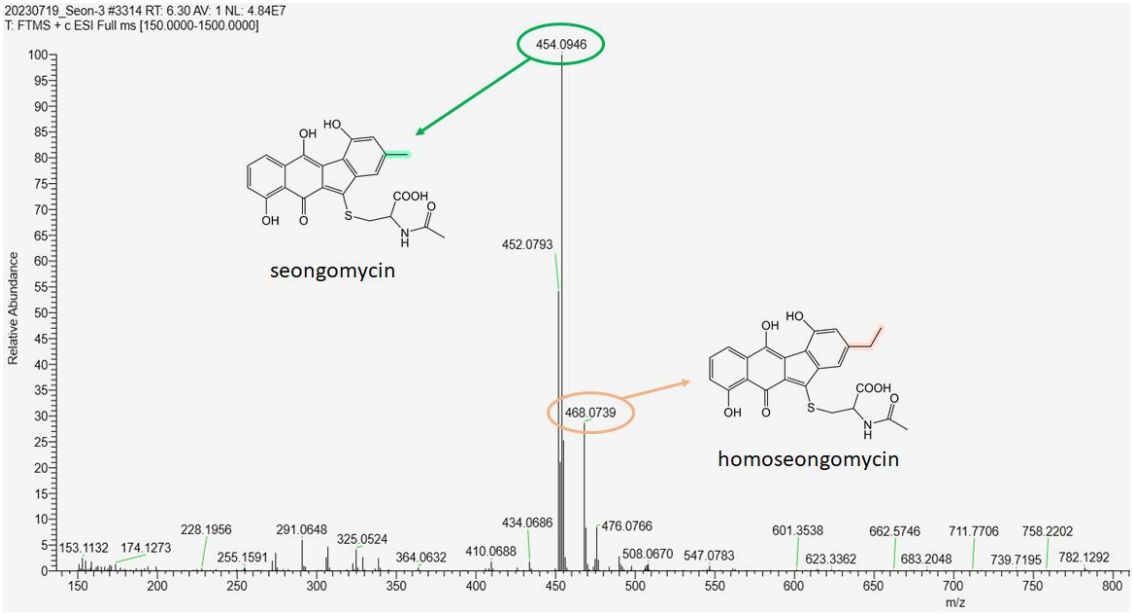

Figure S21. HR-MS/MS spectrum of enriched seongomycin fraction containing molecular ion features of seongomycin and homoseongomycin.

Table S9. NMR data for seongomycin in DMSO-d_6 + 1 drop TFA-*d* and chemical structure including numberings.

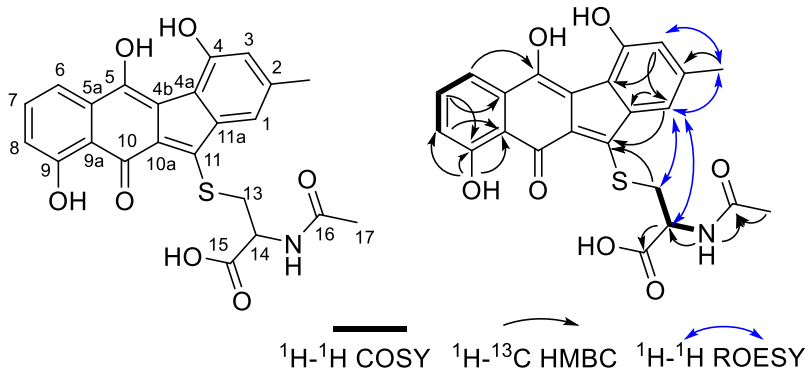

	Experimental data				**Literature reported values by Gould (Tetrahedron Letters, 38, 3139-3142)[14]**	
Position	**δ_C**	**δ_H**	**mult. (*J* in Hz)**	**^{1}H-^{13}C HMBC correlations (default parameters)**	**δ_C**	**δ_H**
1	117.8	7.18	s	11, 11a, 12	117.4	7.12
2	139.0	-			138.7	-
3	117.3	6.76	s	1, 4a	117.1	6.70
4	149.4	-			149.2	-
4a	120.6	-			120.5	-
4b	-	-			114.1	-
5	148.3	-			148.2	-
5a	134.2	-			133.9	-
6	116.4	7.36	dd (7.9; 1.0)	5, 7, 8	116.1	7.30
7	136.4	7.55	t (8.0)	5a, 9	135.9	7.50
8	119.9	6.98	dd (8.0; 1.0)	6, 9a	119.7	6.91
9	163.1	-			163.1	-
9a	116.2	-			116.0	-
9-OH	-	-		8, 9. 9a,	-	13.6
10	-	-			184.0	-
10a	-	-			128.4	-
11	146.7	-		1, 13	146.1	-
11a	142.1	-			141.8	-
12	20.9	2.30	s	1, 3		
13	34.9	3.89 3.55	dd (13.5; 4.7) dd (13.5; 9.0)	11	34.8	3.86 3.53
14	52.6	4.43	dd (8.8; 4.7)	13, 15	52.6	4.43
15	172.0	-			171.9	-
16	169.9	-			169.7	-
17	22.5	1.73	s	16	22.3	1.73
NH	-	8.12	s	14, 16	-	8.23

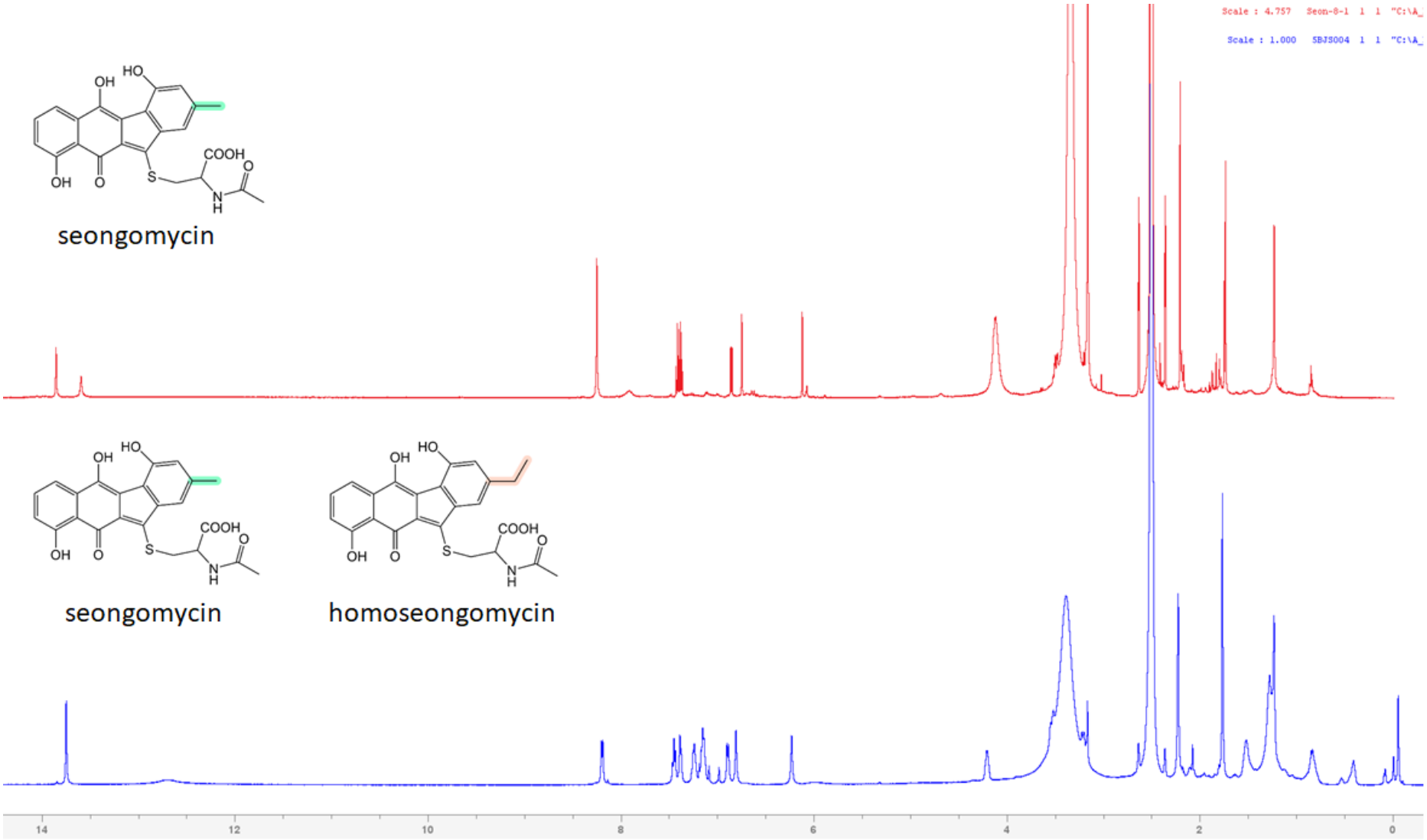

Figure S22. Overlaid ^{1}H NMR spectra of seongomycin (upper spectrum) and a mixture of seongomycin and homoseongomycin in DMSO-d_6 (lower spectrum).

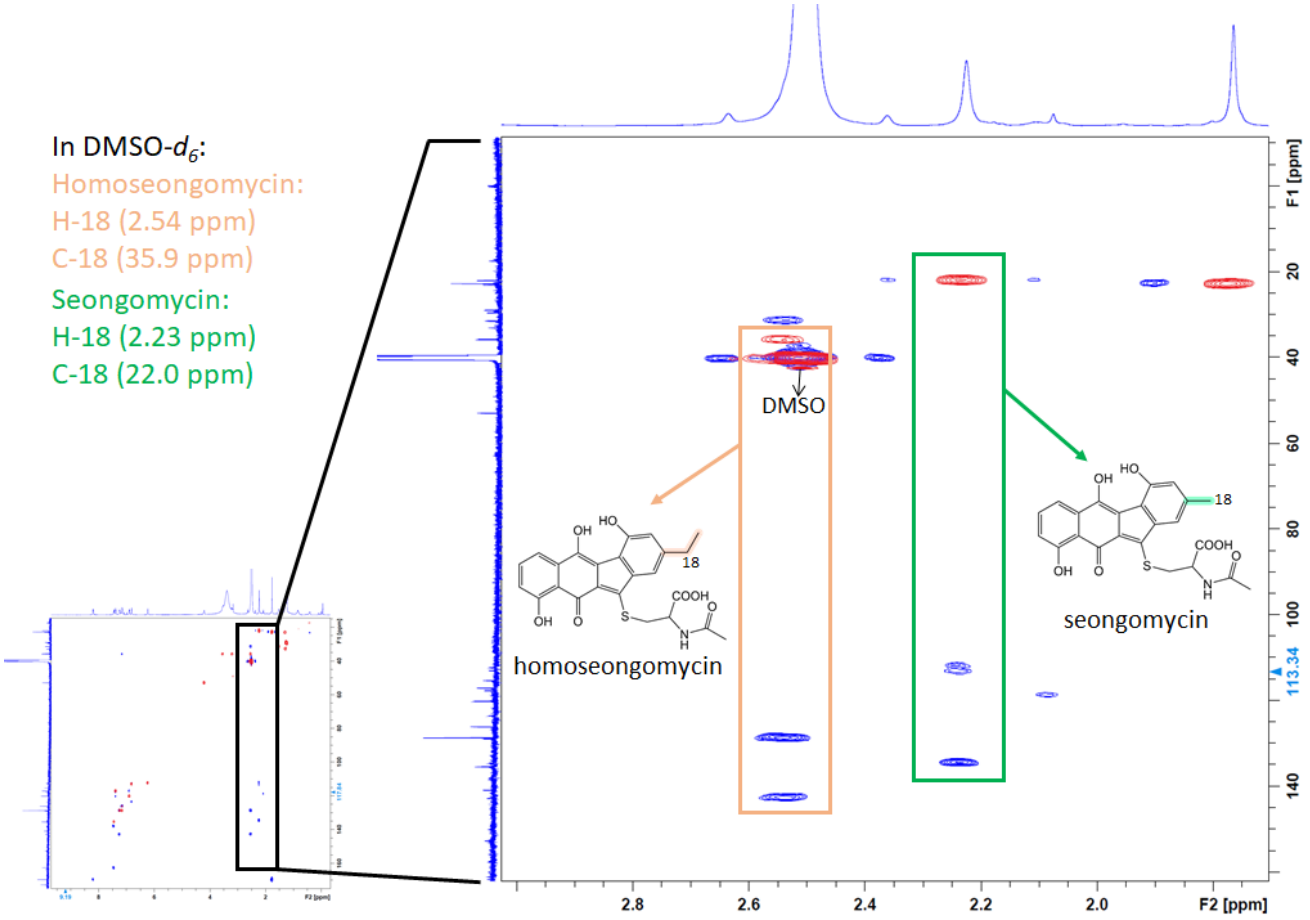

Figure S23. ^{1}H-^{13}C HSQC spectrum of an enriched sample containing seongomycin and homoseongomycin in DMSO-d6.

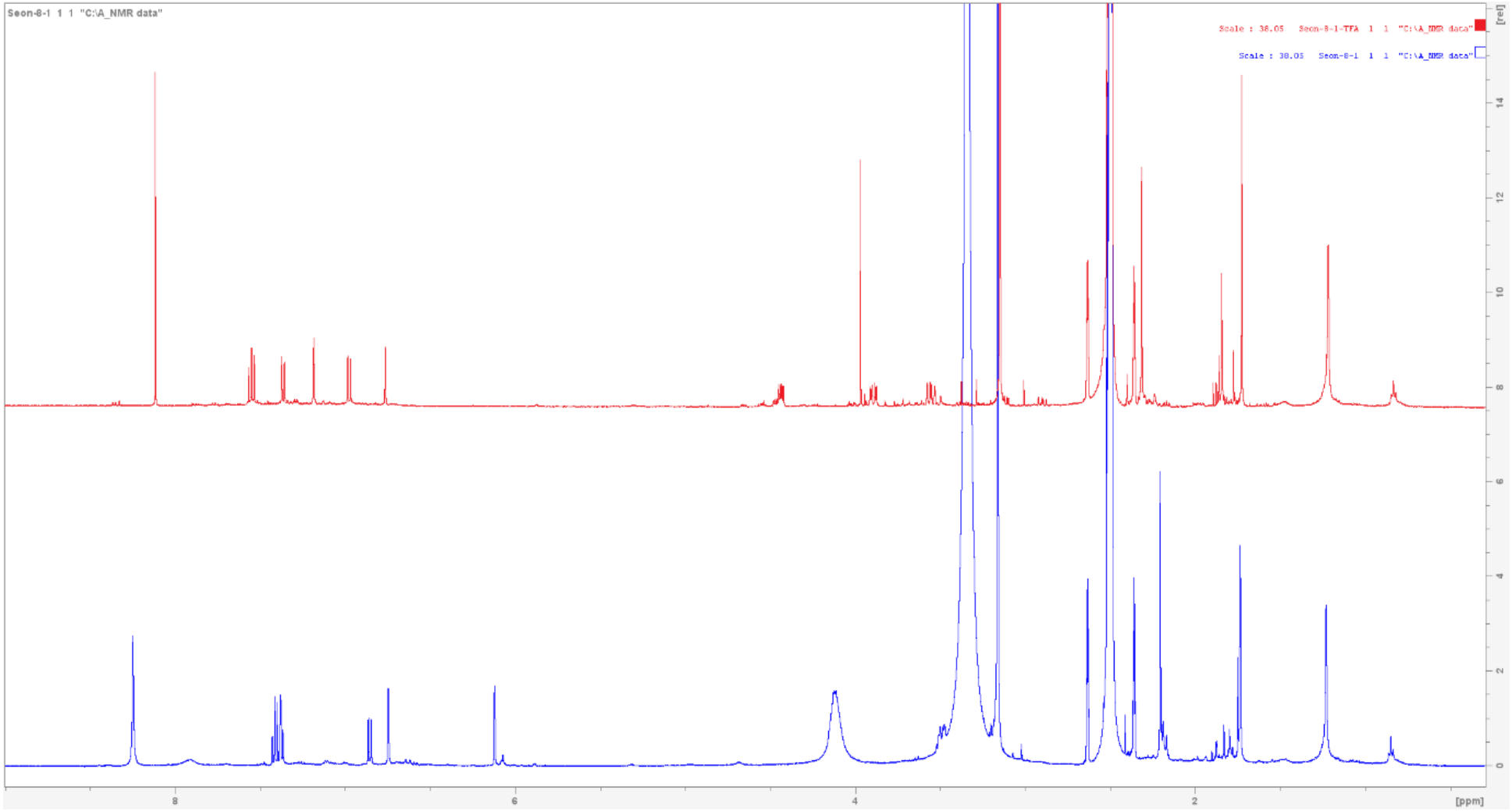

Figure S24. Overlaid ^{1}H NMR spectra of seongomycin in DMSO-d_6 (lower) and DMSO-d_6 + 1 drop TFA-*d* (upper)

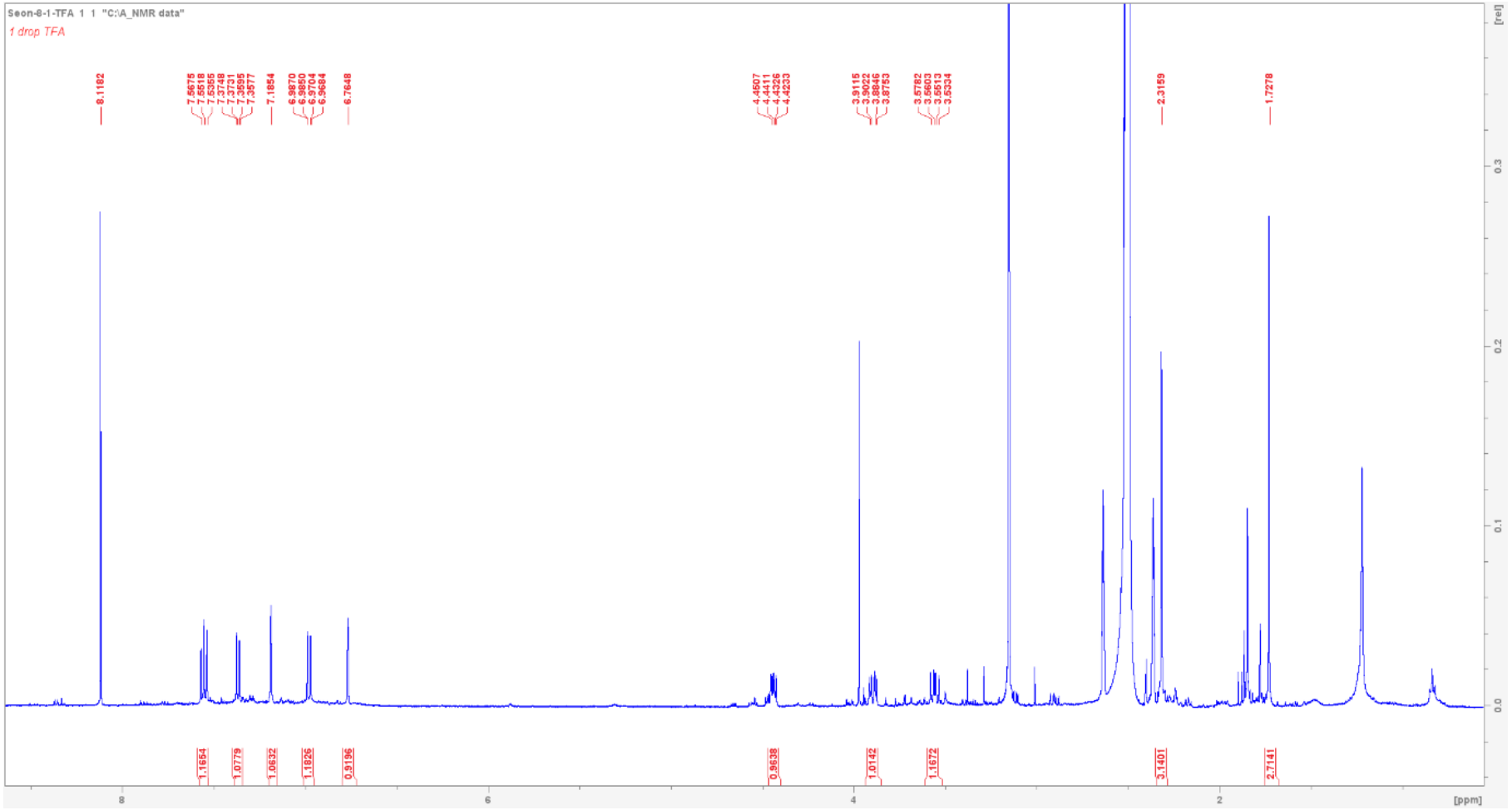

Figure S25. ^{1}H-NMR spectrum of seongomycin in DMSO-d_6 + 1 drop TFA-*d*.

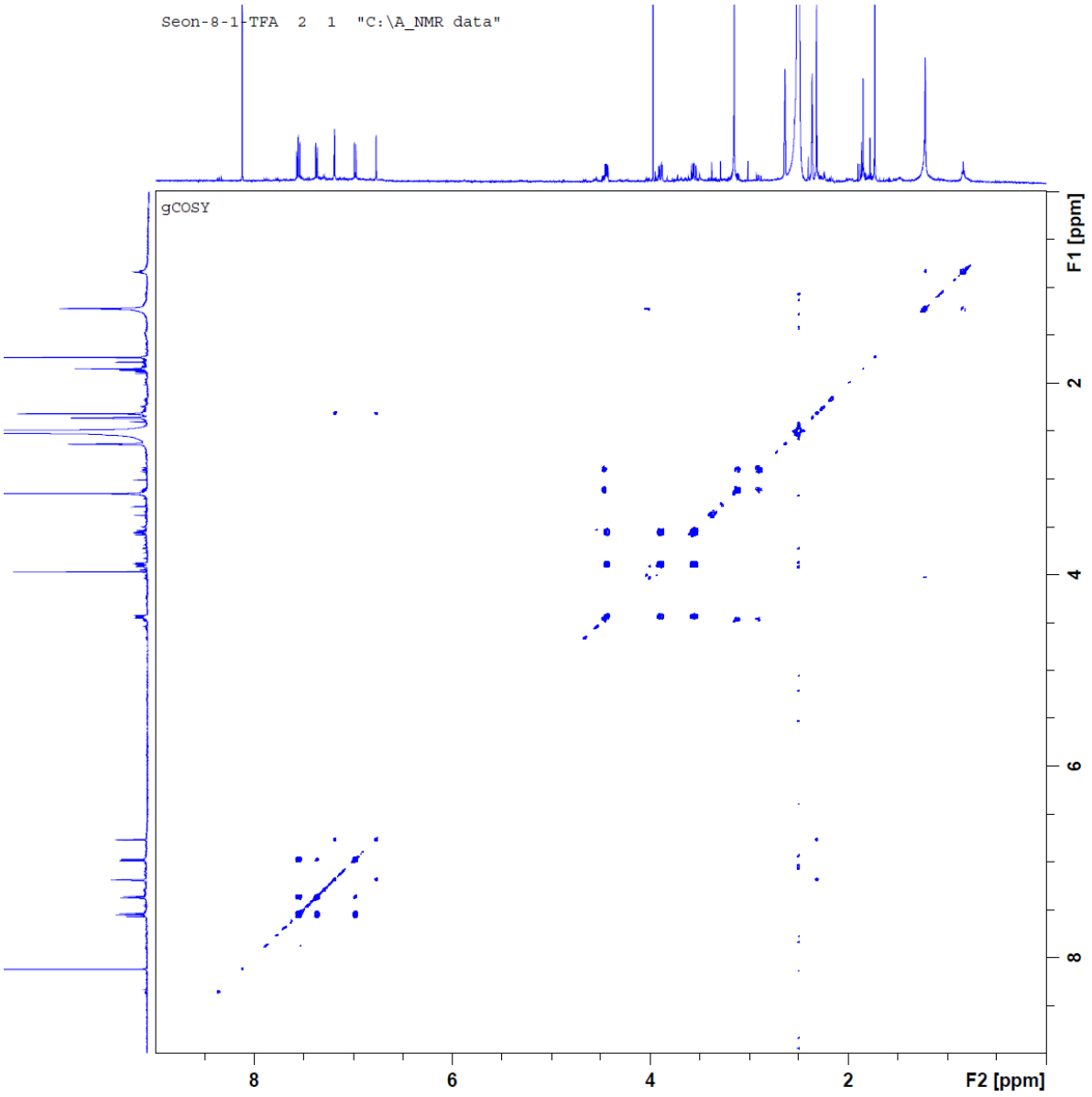

Figure S26. ^{1}H-^{1}H COSY spectrum of seongomycin in DMSO-d_6 + 1 drop TFA-*d*.

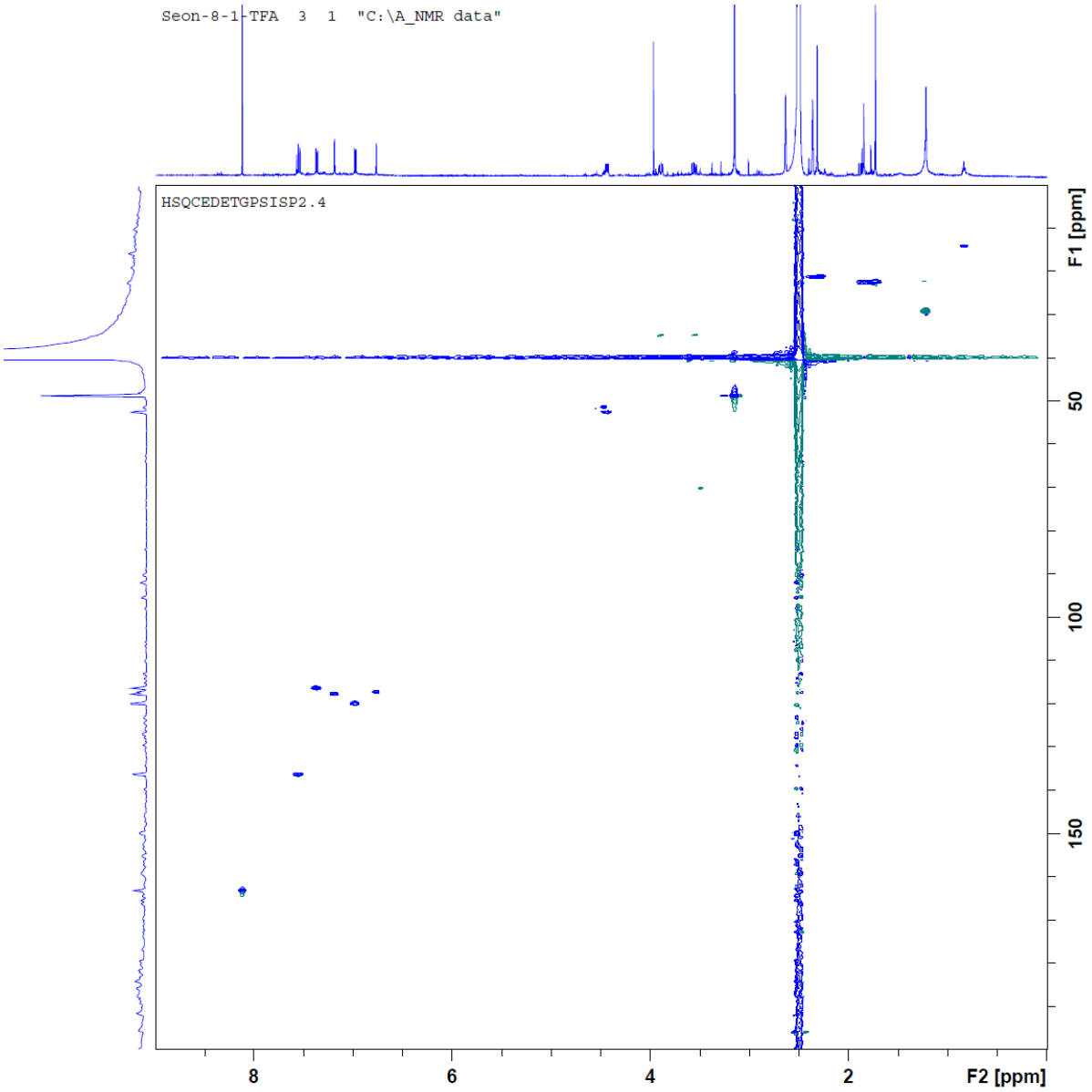

Figure S27. ^{1}H-^{13}C HSQC spectrum of seongomycin in DMSO-d_6 + 1 drop TFA-*d*.

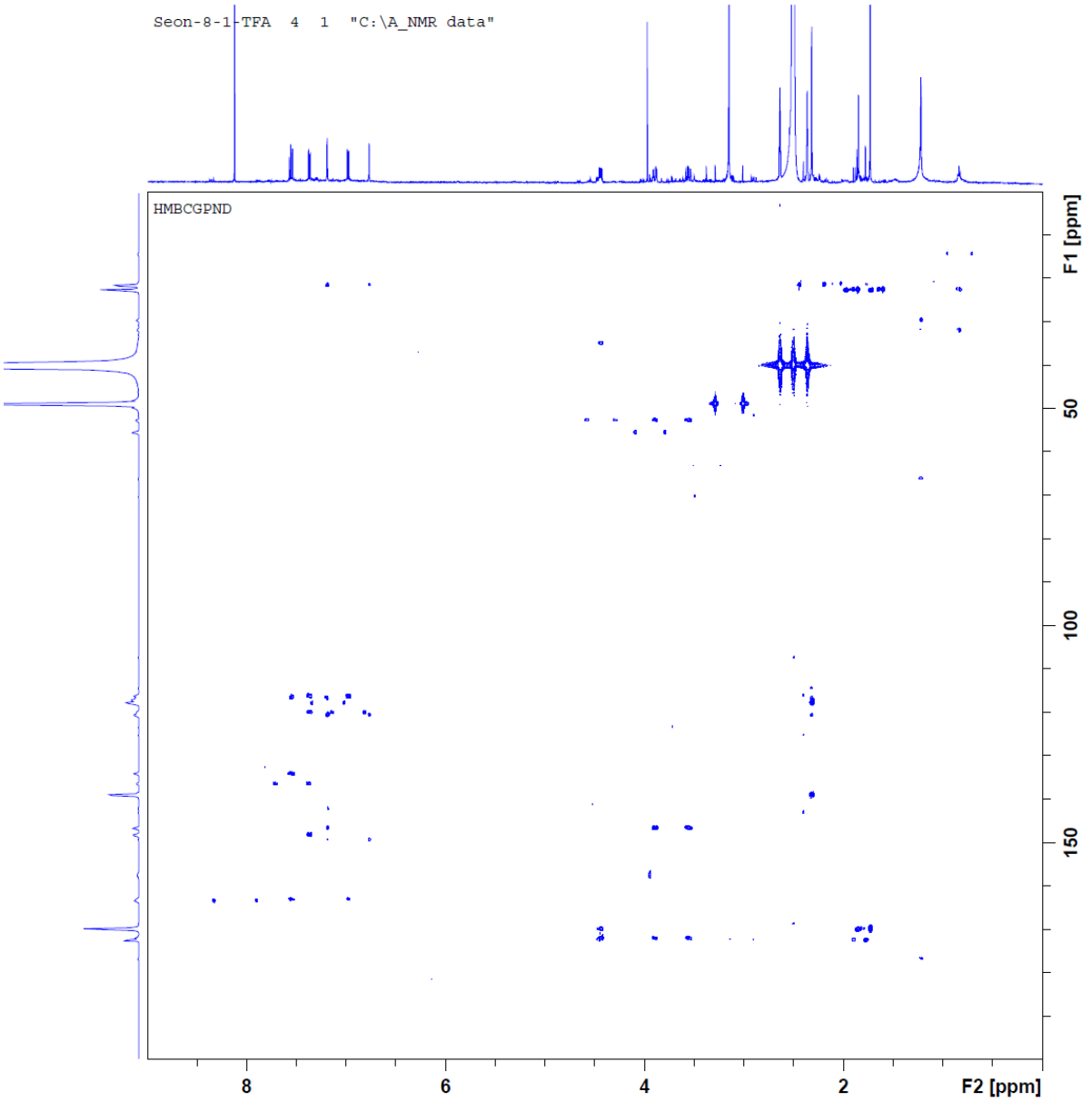

Figure S28. ^{1}H-^{13}C HMBC spectrum of seongomycin in DMSO-d_6 + 1 drop TFA-*d*.

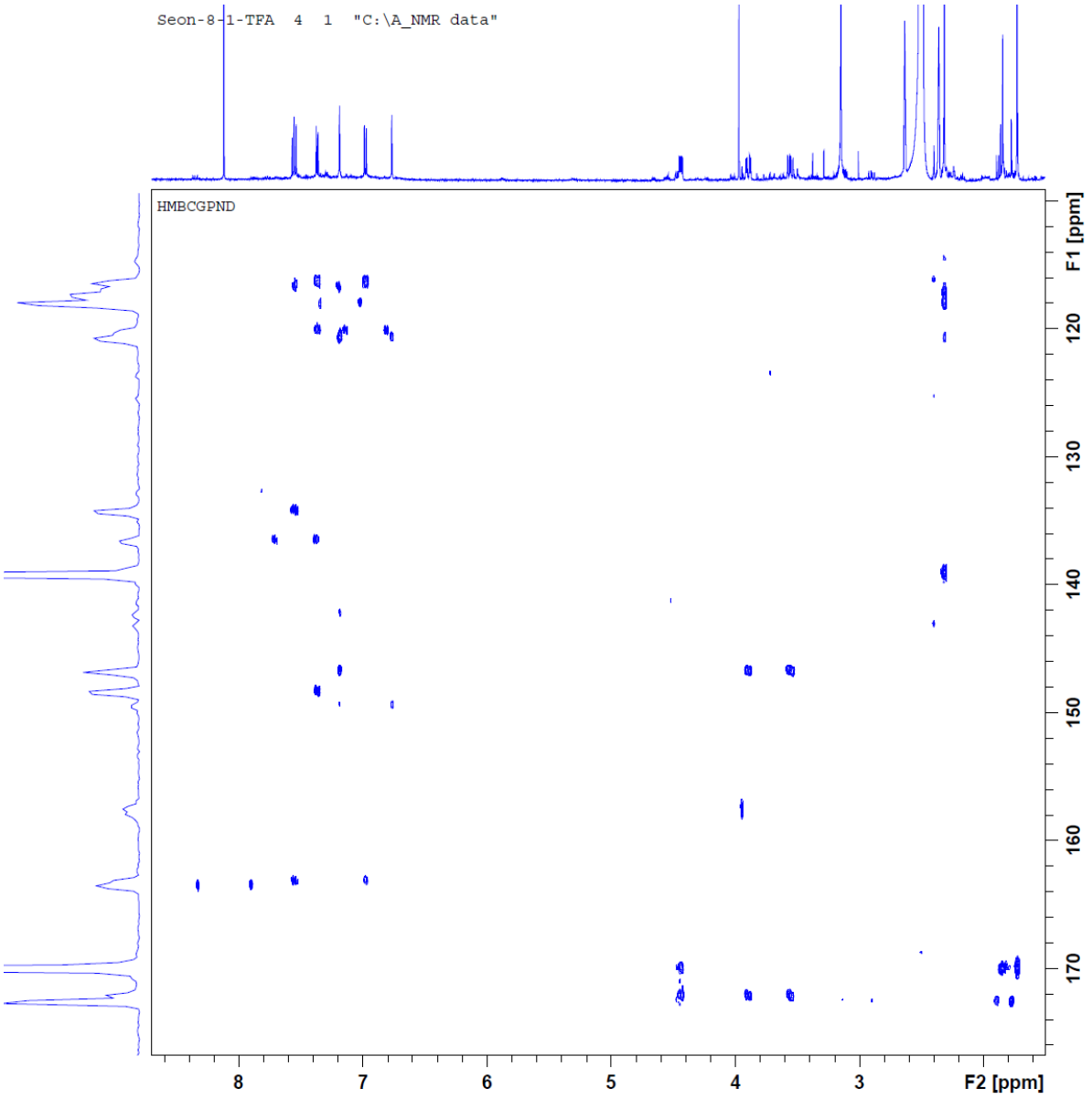

Figure S29. Magnified ^{1}H-^{13}C HMBC spectrum of seongomycin.

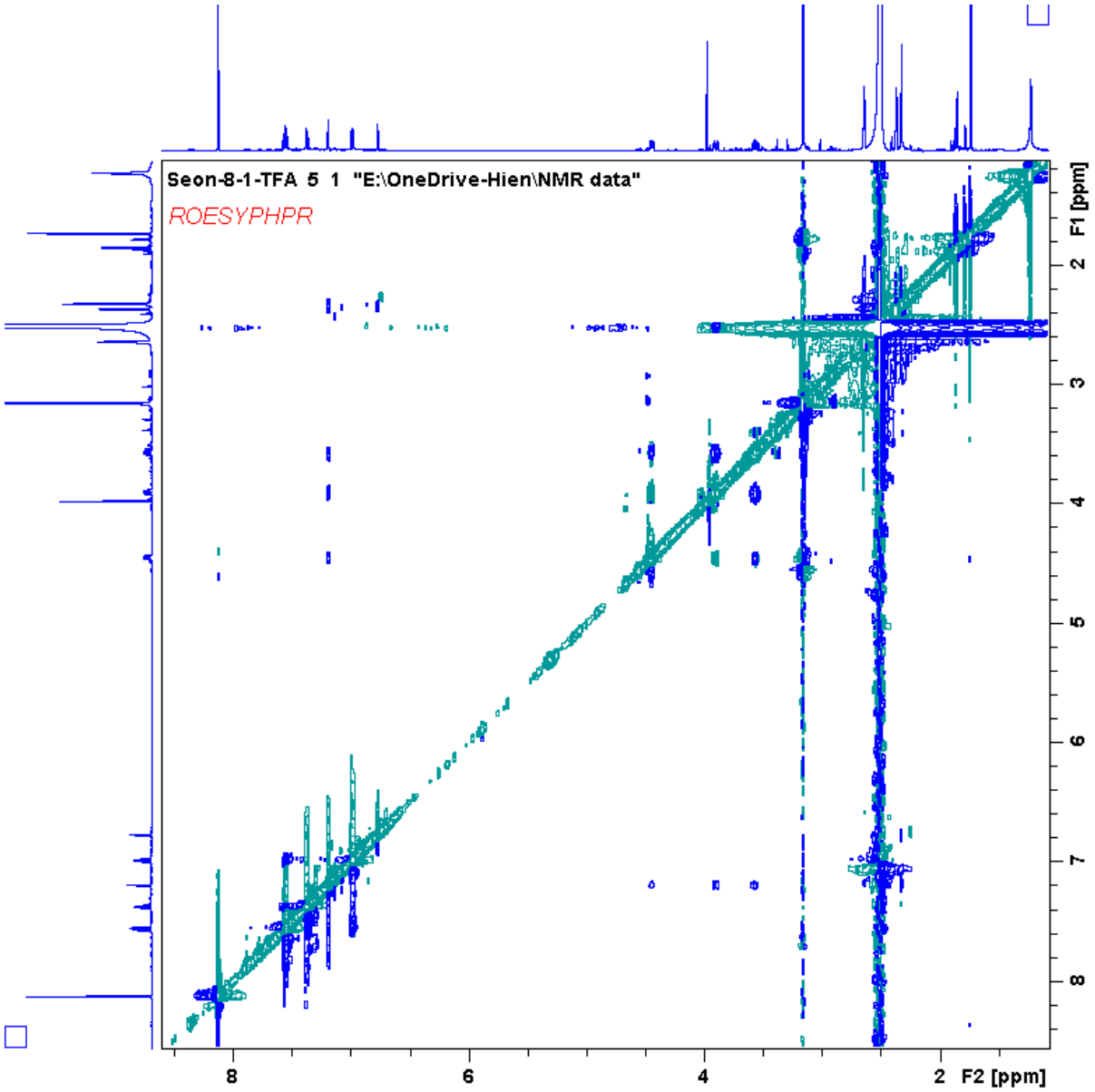

Figure S30. ^{1}H-^{1}H ROESY spectrum of seongomycin in DMSO-d_6 + 1 drop TFA-*d*.

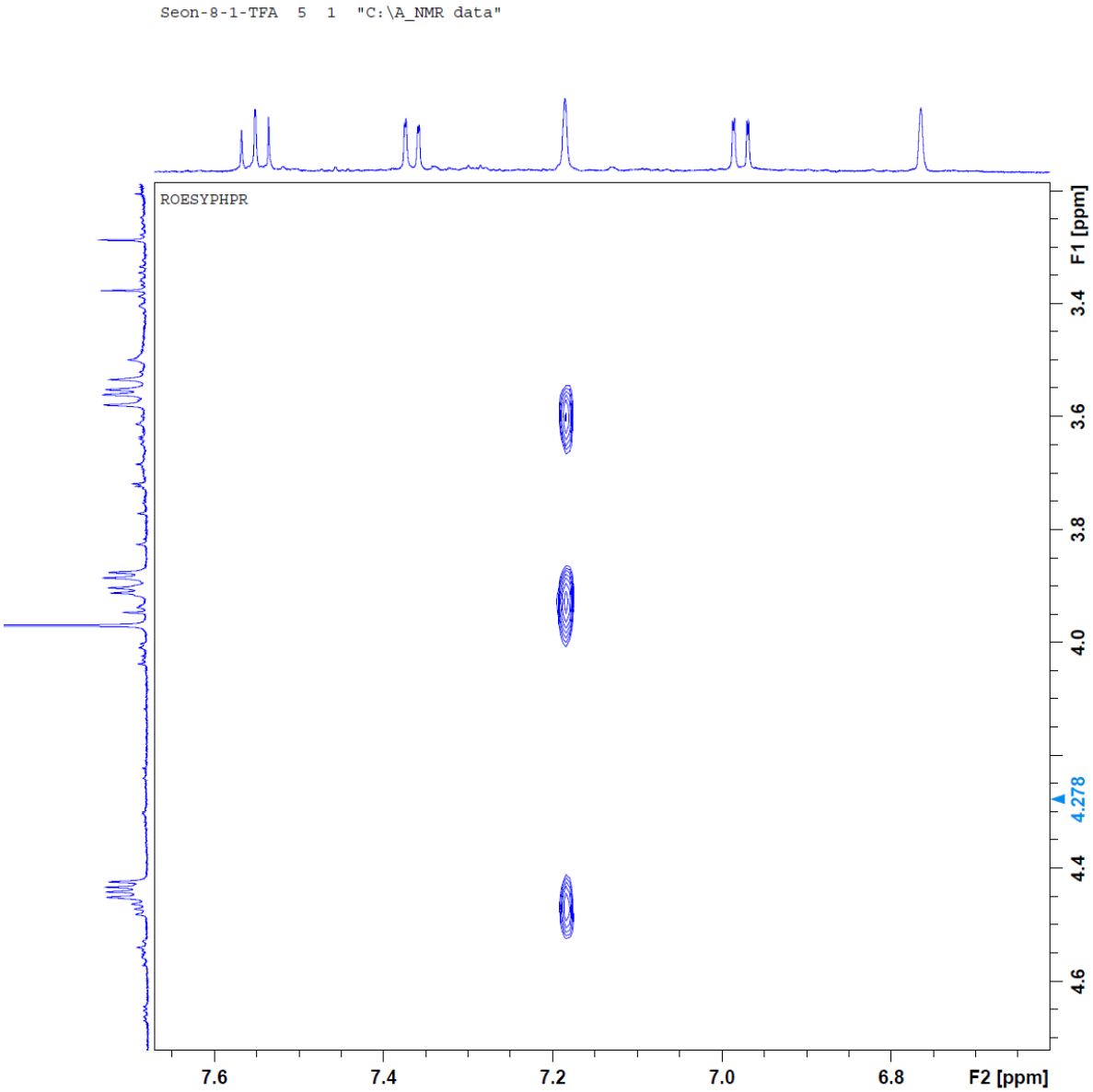

Figure S31. Key ^{1}H-^{13}C ROESY correlations between H-1 (7.18 ppm), H-13 (3.89 and 3.55 ppm) and H-14 (4.43 ppm), confirming the position of H-1 on the aromatic ring.

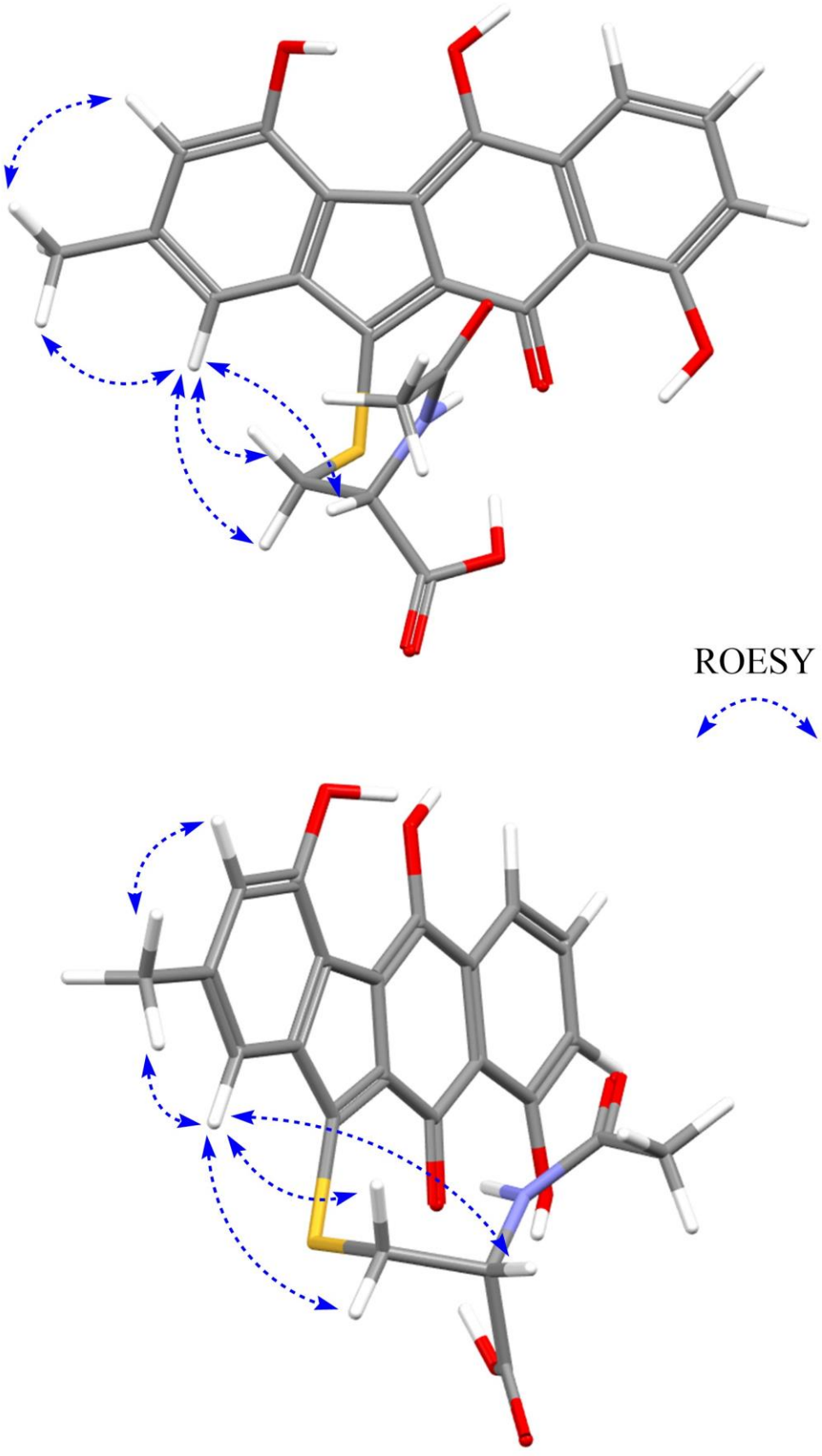

Figure S32. 3D representation of the observed NOE effects for seongomycin.

Table S10. Experimental and calculated ^{1}H and ^{13}C chemical shifts of seongomycin.

Position	Calculated ppm	Experimental ppm	Error Δ ???	Experimental (literature)	Error (literature) Δ ppm
2-CH_3	20.9	21.5	0.6	21.3	0.4
C-4	146.3	149.4	3.1	149.2	2.9
C-3	114.9	117.3	2.4	117.1	2.2
C-2	138.8	139.0	0.2	138.7	0.1
C-1	116.2	117.8	1.6	117.4	1.2
C-4a	117.0	120.6	3,6	120.5	3.5
C-11a	141.5	142.6	1,1	141.8	0.3
C-11	151.0	146.7	4.3	146.1	4.9
C-5	148.8	148.3	0.5	148.2	0.6
C-4b	112.8	-	-	114.1	1.3
C-10a	128.0	-	-	128.4	0.4
C-10	180.6	-	-	184.0	3.4
C-6	114.7	116.4	1.7	116.1	1.4
C-5a	132.0	134.2	2.2	133.9	1.9
C-9a	114.7	116.2	1.5	116.0	1.3
C-9	162.2	163.1	0.9	163.1	0.9
C-8	119.2	119.9	0.7	119.7	0.5
C-7	134.5	136.4	0.9	135.9	1.4
2-CH_3	2.30	2.32	0.02	2.27	0.03
2-CH_3	2.30	2.32	0.02	2.27	0.03
2-CH_3	2.30	2.32	0.02	2.27	0.03
H-3	6.56	6.76	0.2	6.70	0.14
H-1	7.06	7.18	0.12	7.12	0.06
H-6	7.21	7.36	0.15	7.30	0.09
H-8	6.79	6.98	0.19	6.91	0.12
H-7	7.31	7.55	0.24	7.50	0.19

Table S11. Computed and experimental ^{13}C chemical shift values of the revised structure of madural-actomycin A by Guo et al.[15] DFT calculation of ^{13}C chemical shift values of the previously proposed structure pinpoint significant errors at the positions C-8, C-11, C-16, and C-17, indicating an incorrect assignment of the planar structure.

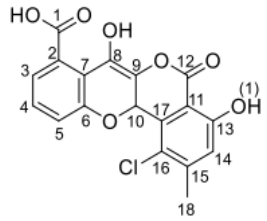

maduralactomycin A (**1**)

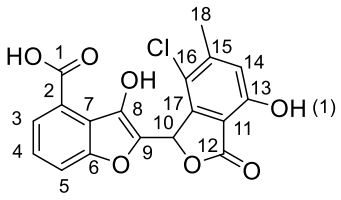

revised maduralactomycin A (**1**)

Position	Calc + Assignment	Exp + Assignment	Error
C-3	127.8	125.6	2.2
C-4	128.2	125.2	3.0
C-5	123.0	115.5	7.5
C-6	152.2	152.5	0.3
C-7	124.9	122.1	2.8
C-2	121.8	127.6	5.8
C-10	66.7	71.8	5.1
C-9	125.5	129.2	3.7
C-8	132.2	141.2	**9.0**
C-17	131.2	145.5	**14.3**
C-11	104.5	117.2	**12.7**
C-12	162.5	166.7	4.2
C-16	130.2	111.7	**18.5**
C-15	149.7	144.6	5.1
C-14	119.5	119.3	0.2
C-13	159.6	155.3	4.3
C-1	169.4	170.1	0.7
15-CH3	22.5	19.6	2.9

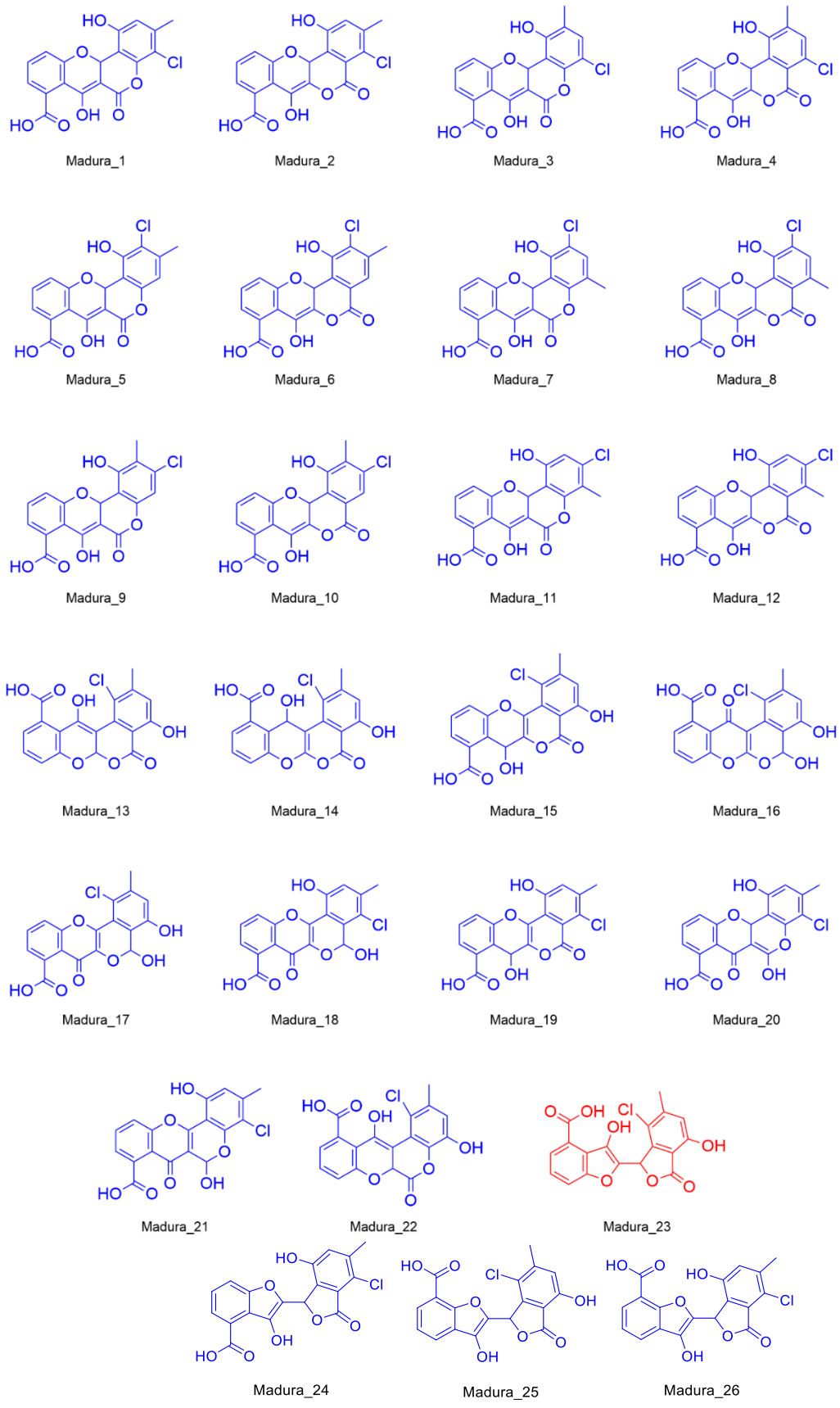

Figure S33. Chemical structures (26) used to compute chemical shifts by extensive DFT calculations.

Table S12. Calculated ^{13}C chemical shifts of the proposed structures named Madura-1 to Madura-12, ranging from the largest to smallest shifts (ppm)

Exp	**Madura-1**	**Madura-2**	**Madura-3**	**Madura-4**	**Madura-5**	**Madura-6**	**Madura-7**	**Madura-8**	**Madura-9**	**Madura-10**	**Madura-11**	**Madura-12**
170.1	167.4	168.8	167.4	168.8	167.3	168.8	167.2	168.9	167.4	168.7	167.4	169.0
166.7	166.3	154.9	166.2	154.6	166.8	157.4	166.8	156.7	166.1	156.8	166.1	156.6
155.3	162.6	152.3	162.4	151.8	163.1	150.6	162.8	150.3	163.0	152.9	162.8	152.1
152.3	155.2	149.8	155.1	149.8	156.3	150.0	156.1	148.5	155.1	150.1	155.1	150.0
145.6	154.0	143.0	153.1	136.7	150.6	140.7	148.9	137.8	154.0	142.7	153.6	142.9
144.7	144.8	133.9	142.9	133.7	147.9	134.3	147.1	133.3	146.5	133.9	147.1	134.3
141.1	142.1	129.6	135.0	133.5	141.2	130.6	134.9	133.1	143.1	130.5	143.4	129.8
129.1	135.1	127.8	132.1	129.7	134.8	127.8	131.3	129.9	134.9	127.9	135.0	128.2
127.6	130.3	127.4	130.3	127.7	129.9	127.5	129.9	128.0	130.3	127.7	130.2	127.4
125.6	124.4	126.9	124.4	127.6	124.0	126.7	124.1	127.5	124.4	126.6	124.4	127.4
125.3	119.9	124.9	123.7	126.5	121.3	123.6	120.3	127.1	121.2	123.4	119.9	124.3
122.1	117.3	123.7	119.9	123.4	120.3	122.6	119.8	124.2	119.9	122.9	117.0	123.6
119.4	116.6	122.3	116.6	122.7	116.9	122.6	119.2	122.0	116.6	121.6	116.6	121.9
117.2	113.3	121.3	116.1	121.1	109.0	121.5	116.9	121.6	108.0	121.2	112.1	121.6
115.6	102.6	119.3	104.5	120.2	102.5	118.9	104.9	121.6	102.4	118.7	102.7	120.8
111.6	86.3	118.3	86.5	115.5	86.4	117.8	86.3	117.7	86.9	117.4	86.4	119.8
71.9	72.1	69.1	72.2	69.1	70.2	68.1	70.6	68.7	72.0	68.7	72.1	69.1
19.6	21.7	22.2	16.6	17.9	21.4	21.2	16.5	24.0	11.9	13.3	12.2	19.5

Table S13. Calculated ^{13}C chemical shifts of the proposed structures Madura-13 to Madura-23, ranging from the largest to smallest shifts (ppm)

Exp	**Madura-13**	**Madura-14**	**Madura-15**	**Madura-16**	**Madura-17**	**Madura-18**	**Madura-19**	**Madura-20**	**Madura-21**	**Madura-22**	**Madura-23**
170.1	170.9	167.3	167.5	174.6	169.6	168.7	167.2	179.6	172.5	171.2	170.3
166.7	165.8	161.8	163.1	163.9	162.7	162.5	156.2	167.5	162.3	164.2	169.3
155.3	159.0	160.3	159.6	162.3	153.6	153.2	150.2	164.4	156.9	154.2	154.1
152.3	152.3	152.3	151.2	151.5	149.9	152.4	147.8	156.4	154.3	144.7	151.1
145.6	148.0	151.7	148.6	149.2	148.1	148.3	142.6	154.0	153.7	141.0	148.6
144.7	146.4	147.1	136.0	142.3	142.7	146.4	134.1	143.3	150.0	135.5	142.1
141.1	134.8	134.1	133.6	133.1	134.7	134.0	133.8	142.1	148.0	133.3	141.5
129.1	129.4	128.8	128.0	131.8	133.7	132.4	133.8	135.3	134.1	129.3	130.3
127.6	129.1	128.0	127.8	131.7	132.3	131.8	128.3	132.6	133.3	128.1	127.4
125.6	128.1	125.9	127.2	128.2	131.3	131.3	128.1	125.2	132.3	127.4	124.4
125.3	124.5	125.4	125.6	125.9	128.5	129.6	126.1	120.4	122.6	124.0	123.9
122.1	122.4	124.0	123.9	122.2	123.7	128.5	124.6	120.1	121.8	122.3	121.9
119.4	118.3	122.2	123.9	122.1	121.9	122.7	124.0	117.9	118.7	122.0	118.7
117.2	116.8	114.9	123.3	115.6	121.4	121.5	122.3	114.4	111.0	119.1	118.6
115.6	107.6	103.8	117.9	114.8	121.2	119.3	117.6	103.4	108.3	115.1	117.6
111.6	98.6	91.4	105.0	100.3	117.2	106.2	115.6	84.3	99.1	95.8	110.0
71.9	96.6	58.7	60.6	94.5	91.6	89.3	60.0	70.5	88.9	72.8	74.4
19.6	22.6	24.0	23.7	22.0	22.1	22.2	22.6	21.6	22.3	21.4	21.7

Table S14. Errors between experimental and calculated chemical shifts of the proposed structures Madura-1 to Madura-12 (ppm)

Error	**Madura-1**	**Madura-2**	**Madura-3**	**Madura-4**	**Madura-5**	**Madura-6**	**Madura-7**	**Madura-8**	**Madura-9**	**Madura-10**	**Madura-11**	**Madura-12**
	2.7	1.3	2.7	1.3	2.8	1.3	2.9	1.2	2.7	1.4	2.7	1.1
	0.4	11.8	0.5	12.1	0.1	9.3	0.1	10.0	0.6	9.9	0.6	10.1
	7.3	3.0	7.1	3.5	7.8	4.7	7.5	5.0	7.7	2.4	7.5	3.2
	2.9	2.5	2.8	2.5	4.0	2.3	3.8	3.8	2.8	2.2	2.8	2.3
	8.4	2.6	7.5	8.9	5.0	4.9	3.3	7.8	8.4	2.9	8.0	2.7
	0.1	10.8	1.8	11.0	3.2	10.4	2.4	11.4	1.8	10.8	2.4	10.4
	1.0	11.5	6.1	7.6	0.1	10.5	6.2	8.0	2.0	10.6	2.3	11.3
	6.0	1.3	3.0	0.6	5.7	1.3	2.2	0.8	5.8	1.2	5.9	0.9
	2.7	0.2	2.7	0.1	2.3	0.1	2.3	0.4	2.7	0.1	2.6	0.2
	1.2	1.3	1.2	2.0	1.6	1.1	1.5	1.9	1.2	1.0	1.2	1.8
	5.4	0.4	1.6	1.2	4.0	1.7	5.0	1.8	4.1	1.9	5.4	1.0
	4.8	1.6	2.2	1.3	1.8	0.5	2.3	2.1	2.2	0.8	5.1	1.5
	2.8	2.9	2.8	3.3	2.5	3.2	0.2	2.6	2.8	2.2	2.8	2.5
	3.9	4.1	1.1	3.9	8.2	4.3	0.3	4.4	9.2	4.0	5.1	4.4
	13.0	3.7	11.1	4.6	13.1	3.3	10.7	6.0	13.2	3.1	12.9	5.2
	25.3	6.7	25.1	3.9	25.2	6.2	25.3	6.1	24.7	5.8	25.2	8.2
	0.2	2.8	0.3	2.8	1.7	3.8	1.3	3.2	0.1	3.2	0.2	2.8
	2.1	2.6	3.0	1.7	1.8	1.6	3.1	4.4	7.7	6.3	7.4	0.1
CMAE*	**5.0**	**3.9**	**4.6**	**4.0**	**5.0**	**3.9**	**4.5**	**4.5**	**5.5**	**3.9**	**5.6**	**3.9**
MAE*	**25.3**	**11.8**	**25.1**	**12.1**	**25.2**	**10.5**	**25.3**	**11.4**	**24.7**	**10.8**	**25.2**	**11.3**

Table S15. Errors between experimental and calculated chemical shifts of the proposed structures Madura-13 to Madura-23 (ppm)

Error			**Madura-13**	**Madura-14**	**Madura-15**	**Madura-16**	**Madura-17**	**Madura-18**	**Madura-19**	**Madura-20**	**Madura-21**	**Madura-22**	**Madura-23**
			0.8	2.8	2.6	4.5	0.5	1.4	2.9	9.5	2.4	1.1	0.2
			0.9	4.9	3.6	2.8	4.0	4.2	10.5	0.8	4.4	2.5	2.6
			3.7	5.0	4.3	7.0	1.7	2.1	5.1	9.1	1.6	1.1	1.2
			0.0	0.0	1.1	0.8	2.4	0.1	4.5	4.1	2.0	7.6	1.2
			2.4	6.1	3.0	3.6	2.5	2.7	3.0	8.4	8.1	4.6	3.0
			1.7	2.4	8.7	2.4	2.0	1.7	10.6	1.4	5.3	9.2	2.6
			6.3	7.0	7.5	8.0	6.4	7.1	7.3	1.0	6.9	7.8	0.4
			0.3	0.3	1.1	2.7	4.6	3.3	4.7	6.2	5.0	0.2	1.2
			1.5	0.4	0.2	4.1	4.7	4.2	0.7	5.0	5.7	0.5	0.2
			2.5	0.3	1.6	2.6	5.7	5.7	2.5	0.4	6.7	1.8	1.2
			0.8	0.1	0.3	0.6	3.2	4.3	0.8	4.9	2.7	1.3	1.4
			0.3	1.9	1.8	0.1	1.6	6.4	2.5	2.0	0.3	0.2	0.2
			1.1	2.8	4.5	2.7	2.5	3.3	4.6	1.5	0.7	2.6	0.7
			0.4	2.3	6.1	1.6	4.2	4.3	5.1	2.8	6.2	1.9	1.4
			8.0	11.8	2.3	0.8	5.6	3.7	2.0	12.2	7.3	0.5	2.0
			13.0	20.2	6.6	11.3	5.6	5.4	4.0	27.3	12.5	15.8	1.6
			24.7	13.2	11.3	22.6	19.7	17.4	11.9	1.4	17.0	0.9	2.5
			3.0	4.4	4.1	2.4	2.5	2.6	3.0	2.0	2.7	1.8	2.1
CMAE*			**4.0**	**4.8**	**3.9**	**4.5**	**4.4**	**4.4**	**4.8**	**5.6**	**5.4**	**3.4**	**1.4**
MAE*			**24.7**	**20.2**	**11.3**	**22.6**	**19.7**	**17.4**	**11.9**	**27.3**	**17.0**	**15.8**	**3.0**

*CMAE = Computed mean absolute error

*MAE = Maximum absolute error

Table S16. Calculated ^{13}C chemical shifts and errors of the proposed structures Madura-23 to Madura-26, ranging from the largest to smallest shifts (ppm) and calculated errors between experimental and calculated chemical shifts of the proposed structures Madura-13 to Madura-23 (ppm).

Exp	**Madura-23**	**Madura-24**	**Madura-25**	**Madura-26**	**Errors-23**	**Errors-24**	**Errors-25**	**Errors-26**
170.1	170.3	169.6	170.2	165.6	**0.2**	0.5	1.8	4.5
166.7	169.3	166.5	163.5	163.7	**2.6**	0.2	3.6	3.0
155.3	154.1	150.6	154.1	149.6	**1.2**	4.7	1.8	5.7
152.3	151.1	148.3	149.7	148.4	**1.2**	4.0	3.6	3.9
145.6	148.6	141.6	148.8	142.0	**3.0**	4.0	1.8	3.6
144.7	142.1	136.0	142.2	135.6	**2.6**	8.7	3.6	9.1
141.1	141.5	133.5	140.0	132.4	**0.3**	7.7	1.8	8.8
129.1	130.3	130.7	129.8	130.1	**1.2**	1.6	3.6	1.0
127.6	127.4	128.6	129.1	129.7	**0.2**	1.0	1.8	2.1
125.6	124.4	127.4	124.3	128.0	**1.2**	1.8	3.6	2.4
125.3	123.9	123.6	124.0	126.6	**1.4**	1.7	1.8	1.3
122.1	121.9	123.5	121.5	125.4	**0.2**	1.4	3.6	3.3
119.4	118.7	121.9	121.3	122.5	**0.6**	2.6	1.8	3.2
117.2	118.6	121.2	117.6	122.0	**1.3**	3.9	3.6	4.7
115.6	117.6	118.6	111.9	120.1	**2.1**	3.1	1.8	4.6
111.6	110.0	117.2	109.7	111.1	**1.7**	5.5	3.6	0.6
71.9	74.4	70.0	74.7	74.2	**2.5**	1.9	1.8	2.3
19.6	21.7	20.6	21.8	20.6	**2.1**	1.0	3.6	1.0
CMAE*					**1.4**	**3.1**	**1.8**	**3.6**
MAE*					**3.0**	**8.7**	**3.6**	**9.1**

*CMAE = Computed mean absolute error

*MAE = Maximum absolute error

Table S17. Computed and experimental ^{13}C chemical shift values of the revised structure of maduralactomycin A using atom numbering as stated in Tables S12-S16 of the computational approach.

Position	Calc + Assignment	Exp + Assignment	Error (ppm)
C-7	170.3	170.1	0.2
C-8	169.3	166.7	2.6
C-9	154.1	155.3	1.2
C-7a	151.1	152.3	1.2
C-11	148.6	144.7	3.9
C-12a	142.1	141.2	0.9
C-3	141.5	145.6	4.1
C-2	130.3	129.1	1.2
C-5	127.4	125.6	1.8
C-6	124.4	125.3	0.9
C-12	123.9	117.3	6.6
C-3a	121.9	127.6	5.7
C-7	118.7	115.5	3.2
C-4	118.6	122.1	3.5
C-10	117.6	119.3	1.7
C-8a	110.0	111.7	1.7
C-7	74.4	71.9	2.5
11-CH3	21.7	19.6	2.1
H-7	6.49	6.73	0.24
H-5	7.90	7.79	0.11
H-6	7.29	7.34	0.05
H-7	7.38	7.57	0.19
H-10	6.78	6.97	0.19
11-CH_3	2.33	2.32	0.01
11-CH_3	2.33	2.32	0.01
11-CH_3	2.33	2.32	0.01

Table S18. NMR Data (DMSO-d_6, at 300 K) and ^{1}H-^{13}C HMBC correlations (incl. long-range correlations based on modified HMBC pulse sequences) for the revised structure of maduralactomycin A.[a,15]

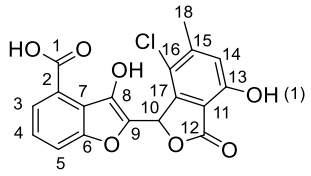

revised maduralactomycin A (**1**)

			maduralactomycin A[15]	
position	δ_C, mult.[b]	δ_H, mult. (*J* in Hz)	^{1}H-^{1}H COSY	^{1}H-^{13}C HMBC (incl. long-range correlations)
1	170.6, qC			
2	127.6, qC			
3	125.5, CH	7.79, d, 7.5	4	1, 4, 5, 6, 7
4	125.2, CH	7.34, t, 7.5	3, 5	2, 3, 6
5	115.2, CH	7.57, d, 7.5	4	4, 6, 7
6	152.6, qC			
7	122.0, qC			
8	141.3, qC			
9	129.0, qC			
10	71.8, CH	6.74, s		8, 9, 11, 12, 13, 16, 17
11	117.2, qC			
12	166.7, qC			
13	155.3, qC			
14	119.2, CH	6.97, s	18	11, 12, 13, 16, 17, 18
15	144.3, qC			
16	111.7, qC			
17	145.5, qC			
18	19.6, CH_3	2.32, s	14	11, 12, 14, 15, 16
OH (1)		11.07, s		13, 14, 16, 17

[a] 600 MHz for ^{1}H NMR and 150 MHz for ^{13}C NMR

[b] numbers of attached protons were determined by analysis of 2D spectra.

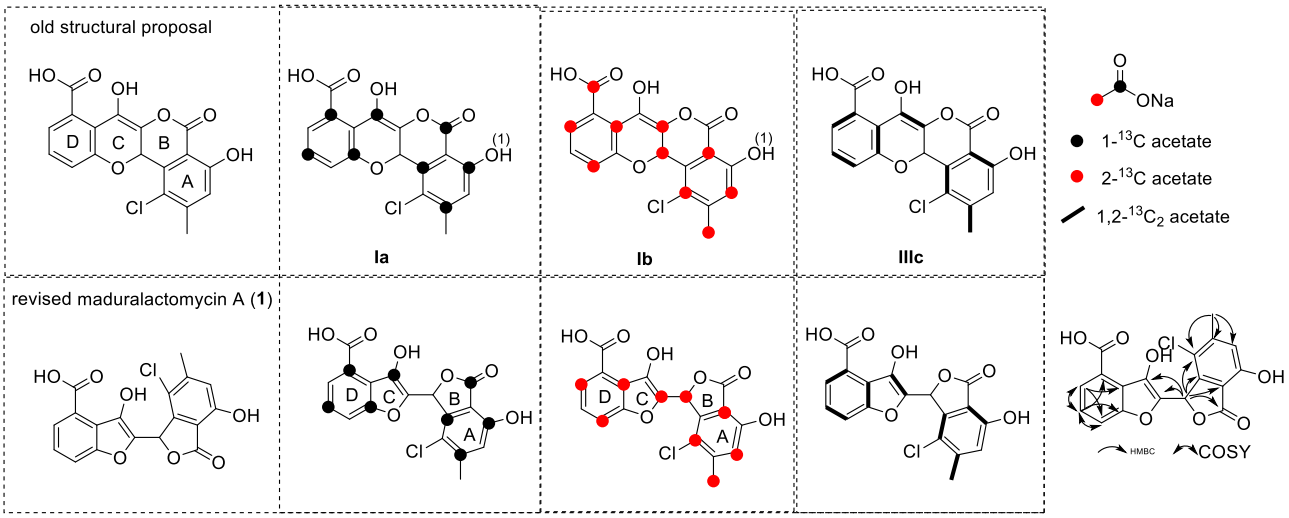

Figure S34. Reassignment of ^{13}C-labeling for revised structure of maduralactomycin.[15] A) 1-^{13}C labeled maduralactomycin A: HRMS analysis showed an increase of the corresponding molecular isotope peak (*m/z* value) that indicated the incorporation of up to eight ^{13}C acetate units. ^{13}C NMR analysis revealed a signal enhancement of C-2, C-4, C-6, C-8, C-12, C-13, C-15 and C-17. B) 2-^{13}C labeled maduralactomycin A: HRMS analysis showed an increase of the corresponding molecular isotope peak (*m/z* value) that indicated the incorporation of up to ten ^{13}C acetate units. ^{13}C NMR analysis of 1b revealed the strong signal enhancement of C-1, C-3, C-5, C-7, C-9, C-10, C-11, C-14, C-16, and C-18. C) 1,2-$^{13}C_2$ labeled maduralactomycin A: HRMS analysis showed an increase of the corresponding molecular isotope peak (*m/z* value) that indicated the incorporation of up to nine or ten ^{13}C acetate units. ^{1}H NMR spectrum was identical with spectra of 1a and 1b. 2D NMR analysis of 1c allowed the assignment of the complete structure. Detailed analysis of ^{13}C NMR revealed the doublet originated from the intact acetate unit, however singlet of C-1, C10, C-12 and C-14 from either rearrangement or decarboxylation.

Table S19. Revised NMR Data (DMSO-d_6, at 300 K) and ^{1}H-^{13}C HMBC correlations (incl. long-range correlations based on modified HMBC pulse sequences) of 1-^{13}C labeled maduralactomycin A (**1a**).[a, 15] HRMS analysis showed an increase of the corresponding molecular isotope peak (*m/z* value) that indicated the incorporation of up to eight ^{13}C acetate units. ^{13}C NMR analysis revealed a signal enhancement of **C-2, C-4, C-6, C-8, C-12, C-13, C-15** and **C-17**.

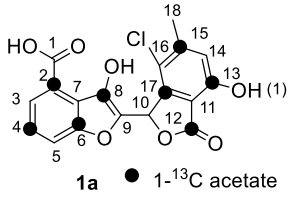

1-^{13}C labeled maduralactomycin A (**1a**) [15]				
position	δ_C, mult.[b]	δ_H, mult. (*J* in Hz)	COSY	HMBC (incl. long-range correlations)
1	**168.9, qC**			
2	132.6, qC			
3	**124.5, CH**	**7.65, d, 7.7**	4	1, 4, 6, 8
4	124.5, CH	7.22, t, 7.7	3, 5	2, 6
5	**113.0, CH**	**7.33, d, 7.7**	4	2, 4, 6
6	152.6, qC			
7	n.d.			
8	142.9, qC			
9	n.d.			
10	**72.4, CH**	**6.66, s**		8, 12, 17
11	**111.8, qC**			
12	167.0, qC			
13	155.7, qC			
14	**119.3, CH**	**6.94, s**	18	11, 12, 13, 16, 17, 18
15	144.4, qC			
16	**116.9, qC**			
17	145.7, qC			
18	**19.6, CH_3**	**2.30, s**	14	15, 16

[a] 600 MHz for ^{1}H NMR and 150 MHz for ^{13}C NMR; red highlight indicated very weak signals.

[b] numbers of attached protons were determined by analysis of 2D spectra.

Table S20. Revised NMR data (DMSO-d_6, at 300 K) and ^{1}H-^{13}C HMBC correlations (incl. long-range correlations based on modified HMBC pulse sequences) of 2-^{13}C labeled maduralactomycin A (**1b**).[a,15] HRMS analysis showed an increase of the corresponding molecular isotope peak (*m/z* value) that indicated the incorporation of up to ten ^{13}C acetate units. ^{13}C NMR analysis of **1b** revealed the strong signal enhancement of **C-1, C-3, C-5, C-7, C-9, C-10, C-11, C-14, C-16, and C-18**.

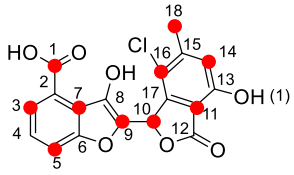

1b ● 2-^{13}C acetate S

2-^{13}C labeled maduralactomycin A (**1b**) [15]				
position	δ_C, mult.[b]	δ_H, mult. (*J* in Hz)	COSY	HMBC (incl. long-range correlations)
1	168.7, qC			
2	**132.6, qC**			
3	124.5, CH	7.64, d, 7.7	4	1, 5, 7
4	n.d.	7.21, t, 7.7	3, 5	2, 3, 6
5	113.0, CH	7.32, d, 7.7	4	3, 7
6	**152.6, qC**			
7	122.5, qC			
8	n.d.			
9	126.9, qC			
10	72.5, CH	6.65, s		9, 11, 16, 17
11	111.8, qC			
12	n.d.			
13	n.d.			
14	119.4, CH	6.93, s		11, 16, 18
15	**144.4, qC**			
16	116.7, qC			
17	**145.7, qC**			
18	19.7, CH_3	2.30, s		14, 15, 16

[a] 600 MHz for ^{1}H NMR and 150 MHz for ^{13}C NMR; red highlight indicated very weak signals.

[b] numbers of attached protons were determined by analysis of 2D spectra.

Table S21. Revised NMR data (DMSO-d_6, at 300 K) and ^{1}H-^{13}C HMBC correlations (incl. long-range correlations based on modified HMBC pulse sequences) of 1,2-$^{13}C_2$ labeled maduralactomycin A (**1c**).[a] HRMS analysis showed an increase of the corresponding molecular isotope peak (*m/z* value) that indicated the incorporation of up to nine or ten ^{13}C acetate units. ^{1}H NMR spectrum was identical with spectra of **1a** and **1b**. 2D NMR analysis of **1c** allowed the assignment of the complete structure. Detailed analysis of ^{13}C NMR revealed the doublet originated from the intact acetate unit, however singlet of C-1, C10, C-12 and C-14 from either rearrangement or decarboxylation.

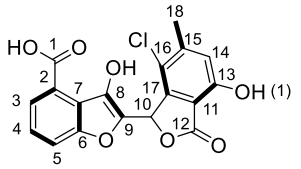

1c 1,2-$^{13}C_2$ acetate

1,2-$^{13}C_2$ labeled maduralactomycin A (**1c**) [15]				
position	δ_C, mult.[b] (*J* in Hz)	δ_H, mult. (*J* in Hz)	COSY	HMBC (incl. long-range correlations)
1	168.9, qC, s			
2	132.5, qC, d (59)			
3	124.4, CH, d, (60)	7.63, d (7.4)	4	1, 5, 7
4	124.1, CH, d (56)	7.18, t (7.8)	3, 5	2, 6
5	112.8, CH, d (58)	7.31, d (8.3)	4	6, 7
6	152.3, qC, d (58)			
7	122.7, qC, d (58)			
8	141.9, qC, d (95)			
9	128.7, qC, d (95)			
10	71.2, CH, s	6.31, s		12, 16, 17
11	109.7, qC, d (64)			
12	**172.1, qC, s**			
13	**171.0, qC, d (64)**			
14	124.7, CH, s	6.17, s	18	11, 12, 16, 18
15	142.4, qC, d (44)			
16	104.3, qC, d (78)			
17	145.0, qC, d (76)			
18	19.8, CH_3, d (44)	2.08, s	14	14, 15, 16
8-OH		16.3, br s		7, 8, 9

[a] 600 MHz for ^{1}H NMR and 150 MHz for ^{13}C NMR; red highlight indicated very weak signals.

[b] numbers of attached protons were determined by analysis of 2D spectra.

Biological Activity Tests

Antimicrobial tests: The activity assay was done by the broth dilution method according to the NCCLS (National Committee for Clinical Laboratory Standards).

Table S22 Antimicrobial activity of seongomycin (1.0 mg/mL in DMSO), ciprofloxacin (5 µg/mL in aqua dest. (cip.) and amphotericin B (10 µg/mL in DMSO/MeOH (amp.) towards Gram (+) and Gram (–) bacteria and fungi.[a]

compd.	*B. subtilis 6633*	*S. aureus SG511*	*E.coli SG458*	*P. aeruginosa SG137*	*MRSA S. aureus 134/94*	*VRSA E. faecalis*	*M. vaccae 10670*	*S. salmonic. 549*	*C. albicans*	*P. notatum JP36*
seongomycin	0	0	0	0	0	0/A	18p	20(p)	12P	14
DMSO (control)	11P	11P	12P	12P	0	11P	11p	12P	0	12p
cip.	27	17	23/31 p	24	0	15F	20p	-	-	-
amp.	-	-	-	-	-	-	-	17p	20	18p

[a]: The value indicated the diameter of inhibition zone (in mm), (p) some colonies in inhibition zone, p colonies in inhibition zone, P many colonies in inhibition zone, A Indication of inhibition, F growth stimulating

Table S23 Minimal inhibitory contentraion (MIC) assay of seongomycin. All used substances were diluted to a concentration of 100 µg/mL. Used solvents and respective MIC of the Test stains are given in the table. All values are given in µg/mL

Substance	Solvent	*C. albicans*	*S. salmonic. 549*	*P. notatum JP36*	*M. vaccae 10670*
Seongomycin	MeOH	50	50	>100	100
Amphotericin B	DMSO/MeOH	0.2	0.1	>100	-
Ciprofloxacin	H_2O	-	-	-	0.2
Solvent control	MeOH	100	100	>100	>100

Cytotoxicity and the antiproliferative activity

Cells and culture conditions for cytological assays: Cells were grown in the appropriate cell culture medium supplemented with 10 mL L-glutamine 1 (CAMBREX 17-605E/U1), 550 µL / L (50 mg/mL) gentamicin sulfate (CAMBREX 17-518Z), and 10 % heat inactivated fetal bovine serum (GIBCO Life Technologies 10270-106) at 37 °C in 5 % CO_2 in high density polyethylene flasks (NUNC 156340).

Proliferation assay: The test substances were dissolved in DMSO before being diluted in cell culture medium. The adherent cells were harvested at the logarithmic growth phase after soft trypsinization using 0.25 % trypsin in PBS containing 0.02 % EDTA (Biochrom KG L2163). For each experiment, approximately 10,000 cells were seeded with 0.1 mL culture medium per well of the 96-well microplates (HUVEC: flat bottomed NUNC 167008, K-562: round bottomed NUNC 163320). To test the antiproliferative effect of natural products on HUVEC and K-562, the cells were incubated for 72 hours in plates prepared with control and different dilutions of test substances. The GI50 values were defined as being where the inhibition of proliferation is 50 % compared to untreated control.

Cytotoxicity assay: For the cytotoxicity assay, HeLa cells were preincubated for 48 hours without the test substances. To test the cytotoxic effect of natural products on HeLa, the dilutions of the compounds were carried out carefully on the subconfluent monolayers of HeLa cells after the preincubation time. After incubation time, the cytolytic effect of compounds were analysed in compare to negative control. The 50 % cytotoxicity concentration (CC50) was defined as the test compound concentration required for destruction in 50 % of the cell monolayer compared to untreated control.

Condition of incubation: The cells were incubated with dilutions of the natural products in microplates for 72 hours at 37 °C in a humidified atmosphere and 5 % CO_2. This incubation was found to be an optimum time for the evaluation of the cytotoxicity and the inhibition of cell proliferation by finding out the number of viable cells stained with CellTiter-Blue® reagent or methylene blue.

Methods of evaluation: For estimating the influence of natural products on cell proliferation of K-562, we determinate the numbers of viable cells present in multiwell plates via CellTiter-Blue® assay (PROMEGA). It uses the indicator dye resazurin to measure the metabolic capacity of cells as indicator of cell viability. Viable cells of untreated control retain the ability to reduce resazurin into resorufin, whereas nonviable cells rapidly lose metabolic capacity and do not reduce the indicator dye. The absorption maximum for resazurin is 605 nm and the absorption maximum for resorufin is 573 nm. Thus, the absorbance measurements at 570 nm and using 600 nm as a reference wavelength can be used to monitor results. Values are compared to blank well containing CellTiter-Blue® reagent without cells. The adherent HUVEC and HeLa cells were fixed by glutaraldehyde (MERCK 1.04239.0250) and stained with a 0.05 % solution of methylene blue (SERVA 29198) for 15 min. After gently washing, the stain was eluted by 0.2 mL of 0.33 N HCl in the wells. The optical densities were measured at 660 nm (methylene blue) in SUNRISE microplate reader (TECAN). Under our experimental conditions, the signals from the methylene blue and CellTiter-Blue® reagent are proportional to the number of viable cells. A repeat determination has been conducted in all experiments, four replicates were assayed. The calculations of the different values of GI50 and CC50 were performed with the software Magellan (TECAN).

Table S24. Used cell lines and cell culture media for cytotoxicity and proliferation assays

Cell line	**Cell culture medium**
HUVEC (ATCC CRL-1730) DMEM	CAMBREX 12-614F
K-562 (DSM ACC 10)	RPMI 1640 (CAMBREX 12-167F)
HeLa (DSM ACC 57)	RPMI 1640 (CAMBREX 12-167F)

Table S25. Antiproliferative and cytotoxic activity test of seongomycin

	Antiproliferative Effect		Cytotoxicity	
HKI- oder sonst. Nr.	HUVEC GI_{50} [µg/ml]	K-562 GI_{50} [µg/ml]	HeLa CC_{50} [µg/ml]	Solubility
Seongomycin	> 50	> 50	20,9 (± 0,7)	DMSO

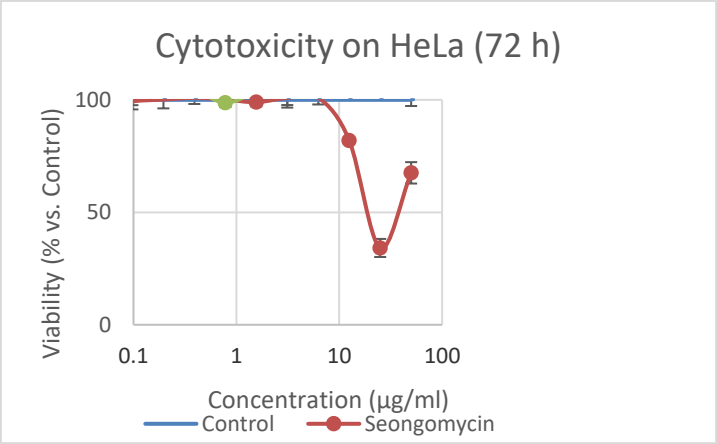

Figure S35. Graphic representation of cytotoxicity of seongomycin. On the Y axis the viability of cells in % and on the X-axis the concentration of the compound is depicted. [16]

Cytotoxicity Assays (Vero E6 and HuH7 5.2 cells)

SEONGOMYCIN (50 – 1.3µM) CYTOTOXICITY PROTOCOL: HuH7 5.2 cells or Vero E6 cells (20,000 cells in 100µL DMEM supplemented with 10% FBS) were seeded directly into each well of a 96 well plate. Cells were incubated at 37 °C, 5% CO_2 with humidified atmosphere for 24h to allow to adherence. Overnight culture media was removed and replaced with 199µL and subsequently treated with 1µL of DMSO-diluted Seongomycin or control substance cis-Diamminplatin(II)-dichlorid (cytotoxic molecule). Cells were incubated with the compounds at 37 °C, 5% CO_2 with humidified atmosphere for 72h before measuring cytotoxicity (cell viability detection) using CellTiter-Glo® Assay. Assay Volume = 200µl; Assay concentration= (50 – 1.3 µM).
SEONGOMYCIN (100 – 0.3µM) CYTOTOXICITY PROTOCOL: HuH7. 5.2 cells or Vero E6 cells (20,000 cells in 100µL DMEM supplemented with 10% FBS) were seeded directly into each well of a 96 well plate. Cells were incubated at 37 °C, 5% CO_2 with humidified atmosphere for 24h to allow to adherence. Overnight culture media was removed and replaced with 100µL of media (DMEM-10% FBS) containing serially diluted compounds (100 – 0.3µM). Cells were incubated with the compounds at 37 °C, 5% CO_2 with humidified atmosphere for 48h before measuring cytotoxicity (cell viability detection) using CellTiter-Glo® Assay. Assay Volume = 90µl; Assay concentration= (100 – 0.3µM).

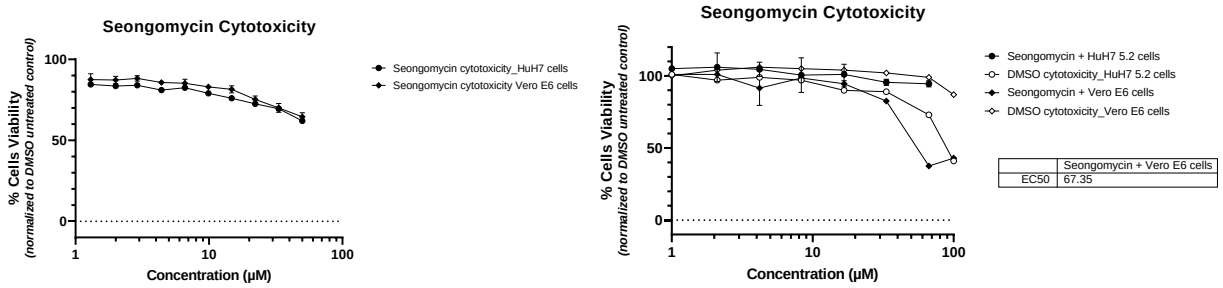

Figure S36. Determination of the C_{50} of seongomycin in HuH7 and Vero E6 cells (67.4 µM in Vero E6 cells; > 100µM in HuH7 5.2 cells).

Antiviral Assays (HuH7 5.2 cells + CHIKV; Vero E6 cells + SARS-CoV2)

SEONGOMYCIN (50 – 1.3µM) PRE-INFECTION & POST INFECTION TREATMENT PROTOCOL: HuH7 5.2 cells or Vero E6 cells (20,000 cells in 194µL DMEM supplemented with 10% FBS) were seeded directly into each well of a 96 well plate. Cells were incubated at 37 °C, 5% CO_2 with humidified atmosphere for 24h to allow to adherence. Cells were treated with 1µL Seongomycin diluted in 100% DMSO or control compounds (Ribavirin for CHIKV screen and Paxlovid or Remdesivir for SARS-CoV2 screen) in 10-dose response to yield assay concentration in the range (50 – 1.3µM) or mock-treated with 1µL of media containing the same concentration of DMSO (post-infection treatment condition). Cells were incubated for 1-2h with the compounds before infection. Subsequently, cells were infected by adding 5µL of virus inoculum (CHIKV or SARS-CoV2 diluted in media to yield MOI 0.1) into the pre-incubation media. Cells +/- compounds + virus were incubated for 1h to allow virus infection. The virus inoculum was removed, and the cell monolayer washed twice with warm PBS to remove nonabsorbed virus. Cells in the pre-infection treatment condition and post-infection treatment condition were replenished with 200µL and 199µL DMEM supplemented with 10% FBS respectively. Cells in the post-infection treatment condition were subsequently treated with 1µL of the test compounds in 10-dose response (50 – 1.3µM).

Plate(s) were incubated at 37 °C, 5% CO_2 with humidified atmosphere for 72h before measuring virus infectivity (cell viability detection) using CellTiter-Glo Assay. Assay Volume = 200µl; Assay concentration= (50 - 1.3 µM).

SEONGOMYCIN (100 – 0.3µM) PRE-INFECTION and POST INFECTION TREATMENT PROTOCOL: HuH7. 5.2 cells (20,000 cells in 100µL DMEM supplemented with 10% FBS) were seeded directly into each well of a 96 well plate. Cells were incubated at 37 °C, 5% CO_2 with humidified atmosphere for 24h to allow to adherence. Overnight culture media was removed, and cells in the pre-infection treatment condition replenished with 45µL of media (DMEM-10% FBS) containing Seongomycin or control compounds (Ribavirin or Chloroquine) serially diluted in media without DMSO in 10-dose response (100 – 0.3 µM). Alternatively, cells in thepost-infection treatment condition were replenished with media containing DMSO serially diluted in media supplemented with 10% FBS in 10-dose response (1 – 0.003%). Cells were incubated with the compounds for 1-2h before infection. Subsequently, cells were infected by adding 5µL of virus inoculum (CHIKV diluted in FBS-free media to yield MOI 0.1) into the pre-incubation media. Cells +/- compounds + virus were incubated for 1h to allow virus infection. The virus inoculum was removed, and the cell monolayer washed twice with warm PBS to remove nonabsorbed virus. Cells in the pre-infection treatment condition were replenished with 90µL media supplemented with 10% FBS. Subsequently, cells in the post-infection treatment condition were treated by adding 90 µL of media containing Seongomycin or control compounds (Ribavirin or Chloroquine) serially diluted in media without DMSO in 10-dose response (100 – 0.3µM). Plates were incubated at 37 °C, 5% CO_2 with humidified atmosphere for 48h before measuring virus infectivity (cell viability detection) using CellTiter-Glo® Assay (Assay Volume = 90 µl; Assay concentration (100 – 0.3µM)).

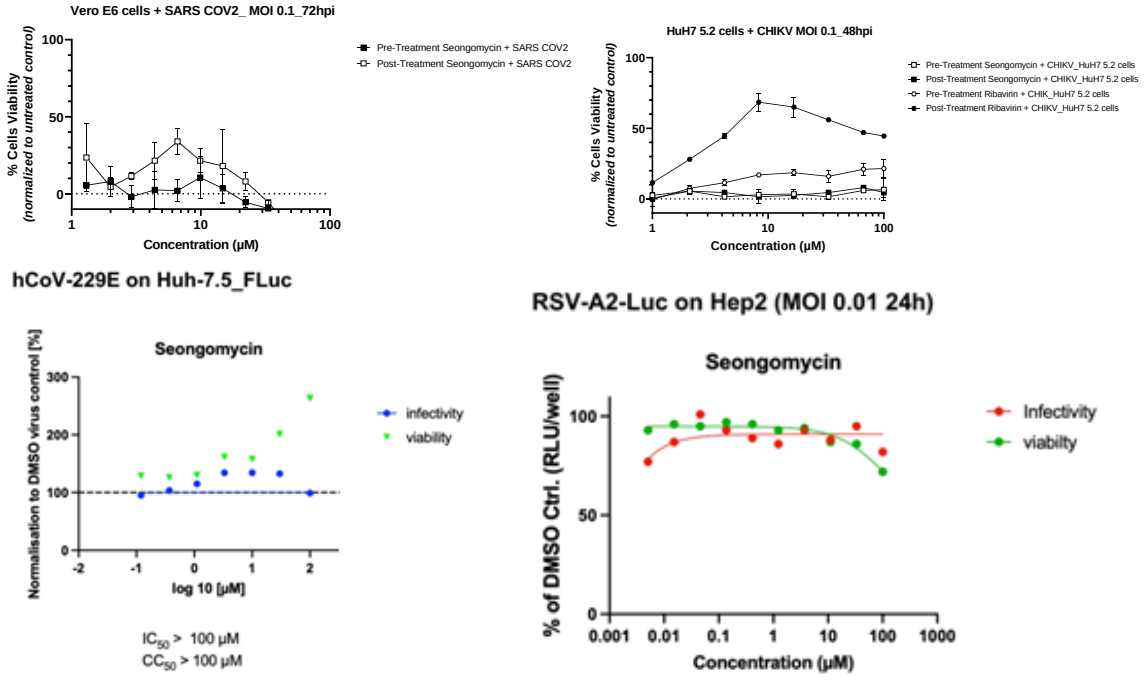

Figure S37. Determination of antiviral activity against SARS-CoV2 or CHIKV when applied to virus-infected cells, either in pre-infection or post-infection treatment conditions.

References

[1] Bilyk, O.; Sekurova, O. N.; Zotchev, S. B.; Luzhetskyy, A., Cloning and heterologous expression of the grecocycline biosynthetic gene cluster. *PloS one* **2016,** *11* (7), e0158682

[2] Shirling, E. B.; Gottlieb, D., Methods for characterization of Streptomyces species. *International Journal of Systematic and Evolutionary Microbiology* **1966,** *16*, 313-340

[3] Chater, K. F.; Wilde, L., Restriction of a bacteriophage of *Streptomyces albus* G involving endonuclease SalI. *Journal of bacteriology* **1976,** *128* (2), 644-650.

[4] Chater, K. F.; Wilde, L. C., *Streptomyces albus* G Mutants Defective in the SalGI Restriction-Modification System. *Microbiology* **1980,** *116* (2), 323-334.

[5] Gomez‐Escribano, J. P.; Bibb, M. J., Engineering *Streptomyces coelicolor* for heterologous expression of secondary metabolite gene clusters. *Microbial biotechnology* **2011,** *4* (2), 207-215.

[6] Hopwood, D. A.; Kieser, T.; Wright, H. M.; Bibb, M. J., Plasmids, Recombination and Chromosome Mapping in *Streptomyces lividans* 66. *Microbiology* **1983,** *129* (7), 2257-2269.

[7] Figurski, D. H.; Helinski, D. R., Replication of an origin-containing derivative of plasmid RK2 dependent on a plasmid function provided in trans. *Proceedings of the National Academy of Sciences* **1979,** *76* (4), 1648-1652.

[8] Ditta, G.; Stanfield, S.; Corbin, D.; Helinski, D. R., Broad host range DNA cloning system for gram-negative bacteria: construction of a gene bank of *Rhizobium meliloti*. *Proceedings of the National Academy of Sciences* **1980,** *77* (12), 7347-7351.

[9] Paget, M. S.; Chamberlin, L.; Atrih, A.; Foster, S. J.; Buttner, M. J., Evidence that the extracytoplasmic function sigma factor ςE is required for normal cell wall structure in *Streptomyces coelicolor* A3 (2). *Journal of bacteriology* **1999,** *181* (1), 204-211.

[10] MacNeil, D. J.; Gewain, K. M.; Ruby, C. L.; Dezeny, G.; Gibbons, P. H.; MacNeil, T., Analysis of *Streptomyces avermitilis* genes required for avermectin biosynthesis utilizing a novel integration vector. *Gene* **1992,** *111* (1), 61-68.

[11] Gust, B.; Challis, G. L.; Fowler, K.; Kieser, T.; Chater, K. F., PCR-targeted Streptomyces gene replacement identifies a protein domain needed for biosynthesis of the sesquiterpene soil odor geosmin. *Proceedings of the National Academy of Sciences* **2003,** *100* (4), 1541-1546.

[12] Gust, B.; Challis, G. L.; Fowler, K.; Kieser, T.; Chater, K. F., PCR-targeted Streptomyces gene replacement identifies a protein domain needed for biosynthesis of the sesquiterpene soil odor geosmin. *Proceedings of the National Academy of Sciences* **2003,** *100* (4), 1541-1546.

[13] Datsenko, K. A.; Wanner, B. L., One-step inactivation of chromosomal genes in *Escherichia coli* K-12 using PCR products. *Proceedings of the National Academy of Sciences* **2000,** *97* (12), 6640-6645.

[14] Carney, J., R.; Hong, S.-Tshool; Gould, S., J., Tetrahedron Letters 1997, 38, 3139-3142.

[15] H. Guo, J. W. Schwitalla, R. Benndorf, M. Baunach, C. Steinbeck, H. Görls, Z. W. de Beer, L. Regestein, C. Beemelmanns, *Org. Lett.* 2020, **22**, 2634-2638.

[16] Zehra A, Hashmi MZ, Khan AM, Malik T, Abbas Z. Biphasic Dose–Response Induced by PCB150 and PCB180 in HeLa Cells and Potential Molecular Mechanisms. *Dose-Response*. 2020;18(1). doi:10.1177/1559325820910040